Supporting Information

# Persilylation of Ferrocene: The Ultimate Discipline in Sterically Overcrowded Metal Complexes

Susanne M. Rupf,[a] Robin Sievers,[a] Paulin S. Riemann,[a] Marc Reimann,[b] Prof. Dr. Martin Kaupp,[b] Dr. Carlo Fasting,[a] Dr. Moritz Malischewski[a*]

[a]Freie Universität Berlin, Fabeckstr. 34-36, 14195 Berlin Germany

[b]Technische Universität Berlin, Straße des 17. Juni 135, 10623 Berlin Germany

E-Mail corresponding author: moritz.malischewski@fu-berlin.de

# 1 General Considerations

Commercially available chemicals were used as received, unless otherwise noted. $[FeC_{10}Br_{10}]$[1,2] was prepared as described previously in literature. Dimethylchlorosilane was freshly distilled over $CaH_2$, degassed and stored in a flame dried Young flask. THF was freshly distilled over Na. *n*-Pentane was received from the solvent system FMBRAUN MB SPS-800. Both solvents were stored in Young flasks under argon atmosphere over molar sieve (3 Å) which was dried beforehand at 250 °C under high vacuum. The glass apparatuses were initially purged with *tert*-BuLi in addition to standard drying methods. $^t$BuLi is an extreme pyrophoric and toxic chemical. The recommended handling and quenching procedures should be strictly followed.[3] Mercury compounds are highly toxic and should only be handled with appropriate safety equipment.

$^1$H, $^{13}$C and $^{29}$Si NMR spectra were recorded on a Bruker AVANCE III 700 spectrometer by using 6mm NMR glass tubes. All reported chemical shifts (δ) are referenced to the Ξ values given in IUPAC recommendations of 2008 using the $^2$H signal of the deuterated solvent as internal reference.[4] All chemical shifts (δ) are given in parts per million (ppm) and the signals are specified according to the multiplicity (s = singlet, d = doublet, t = triplet, q = quartet, m = multiplet, br = broad) and the coupling constants J in Hz. The program MestRe Nova Version 14.0.1 was used to evaluate and plot the data.[5]

Mass spectrometry was performed on a Agilent 6210 ESI TOF (electrospray ionization time-of-flight spectrometer) of Aglient Technologies, Santa Clara, CA in negative mode. Flow rates were set to 10 µL·min$^{-1}$ or using a Varian MAT 711 spectrometer by electron impact ionization (EI) at the department of mass spectroscopy at the Freie Universität Berlin. The evaluation of the resulting data occurred by using Mmass 5.5.0.[6]

Infrared spectra were either measured using a Thermo-Scientific Nicolet iS10 FTIR spectrometer with DuraSamplIR accessory in attenuated total reflection at room temperature. The software OriginPro 2017G was used to plot the data.[7]

The UV/VIS spectra were recorded on a Varian Cary 50 Bio photospectrometer (xenon lamp) in Suprasil glass cuvettes (thickness of 1 cm).

# 2 Experimental Details

List of compounds:

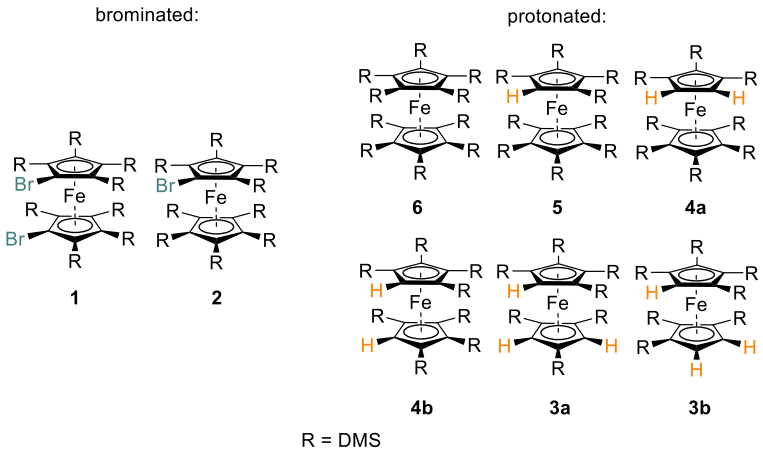


**Silylation – General Procedure via Grignard reaction.** In a dry 50 mL pressure tube magnesium (20 eq.) was placed in anhydrous and degassed THF (2 mL) under an argon atmosphere and was activated with some drops of 1,2-dibromethane. Then DMSCl (30 eq.) and decabromoferrocene (50 mg, 1.0 eq.) were suspended in anhydrous

and degassed THF (15 mL) were added subsequently dropwise and the reaction mixture was stirred for various reaction times at different temperatures:

Table S1. Varied reaction conditions in the reaction of decabromoferrocene with elemental Mg and DMSCl in THF. The corresponding ESI MS spectra are depicted in section 4.4.

| **Enrty** | 1 | 2 | 3 | 4 |
|---|---|---|---|---|
| **Time** | 16h | 2d | 2d | 16h |
| **Temperature** | 60°C | 60°C | room temperature | room temperature |

The suspension was quenched with $H_2O$ at 0°C and extracted with *n*-pentane. The organic layer was dried over $MgSO_4$, filtrated and the organic solvent was removed under reduced pressure to afford a red oil which was used for the mass experiments. The combined samples (using in total 2.3 g of decabromoferrocene) were prepurified with column chromatography [$SiO_2$, *n*-pentane]. The crude product (509 mg) was afforded as a red oil and was further purified by HPLC [RP-18, MeOH/$H_2O$ (98:2) then MeOH]. Several highly silylated ferrocenes could be isolated.

**4a**: 1,2,3,4,5-penta(dimethylsilyl)cyclopentadienyl-1,2,3-tri(dimethylsilyl)cyclopentadienyliron(II): pink solid, 55 mg, 4%. $^1$H NMR ($CDCl_3$, RT, 400 MHz): $\delta$ = 4.66 (hept, $J$ = 3.6 Hz, 7H, Si-H), 4.63 (s, 2H, Cp-H), 4.55 (hept, $J$ = 3.8 Hz, 1H, Si-H), 0.40 (d, $J$ = 3.9 Hz, 30H, Me), 0.38 (d, $J$ = 3.6 Hz, 6H, Me), 0.35 (d, $J$ = 3.8 Hz, 6H, Me), 0.17 (d, $J$ = 3.7 Hz, 6H, Me) ppm. $^{13}$C{$^1$H} NMR ($CDCl_3$, RT, 176 MHz): $\delta$ = 89.9 (s, Cp-C), 83.8 (s, Cp-C), 82.1 (s, Cp-C), 79.0 (s, Cp-C), 0.5 (s, Me), 0.2 (s, Me), -0.0 (s, Me), -1.4 (s, Me). ppm. $^{29}$Si NMR ($CDCl_3$, RT, 80 MHz) $\delta$ = -18.2, -22.2, -25.8 ppm. $\tilde{\nu}$ (cm$^{-1}$) = 2951 ($\nu_{C\text{-}H}$), 2902 ($\nu_{C\text{-}H}$), 2135 ($\nu_{Si\text{-}H}$), 1409, 1247, 1197, 1112, 1024, 992, 945, 867, 827, 778, 758. MS (ESI) cald for $[FeC_{10}DMS_8H_2]^+$: 650.2042. Found: 650.1946. EA: cald. 47.95 (C), 8.98 (H), 0.00 (N), 0.00 (S); found 47.63 (C), 8.90 (H), 0.01 (N), 0.00 (S).

**4b**: Bis(1,2,3,4-tetra(dimethylsilyl)cyclopentadienyl)iron(II): red solid, 80 mg, 5%. $^1$H NMR ($CDCl_3$, RT, 400 MHz): $\delta$ = 4.71 (hept, J = 3.9 Hz, 4H, Si-H), 4.66 (hept, J = 3.9 Hz, 4H, Si-H), 4.43 (s, 2H, Cp-H), 0.43 (m, 24H, Me), 0.32 (d, J = 3.8 Hz, 12H, Me), 0.12 (d, J = 3.6 Hz, 13H, Me).ppm. $^{13}$C{$^1$H} NMR ($CDCl_3$, RT, 176 MHz): $\delta$ = 86.6 (s, Cp-H), 85.4 (s, Cp-C), 82.9 (s, Cp-C), 0.4 (s, Me), 0.1 (s, Me), -0.4 (s, Me), -2.4 (s, Me) ppm. $^{29}$Si NMR ($CDCl_3$, RT, 80 MHz) $\delta$ = -18.0, -21.4 ppm. IR (ATR, RT): $\tilde{\nu}$ (cm$^{-1}$) = 2957 ($\nu_{C\text{-}H}$), 2924 ($\nu_{C\text{-}H}$), 2854 ($\nu_{C\text{-}H}$), 2176 ($\nu_{Si\text{-}H}$), 2141 ($\nu_{Si\text{-}H}$), 1253, 1202, 1113 ($\delta_{C\text{-}H}$), 1080 ($\delta_{C\text{-}H}$), 1023 ($\delta_{C\text{-}H}$), 947, 876, 823, 800, 759, 727, 698, 654, 678. MS (ESI) cald for $[FeC_{10}DMS_8H_2]^+$: 650.2042. Found: 650.1946. EA: cald. 47.95 (C), 8.98 (H), 0.00 (N), 0.00 (S); found 47.59 (C), 8.78 (H), 0.01 (N), 0.00 (S).

**3a**: 1,2,3,4-tetra(dimethylsilyl)cyclopentadienyl-1,2,4-tri(dimethylsilyl)cyclopentadienyliron(II): red solid, 45 mg, 3%. $^1$H NMR ($CDCl_3$, RT, 400 MHz): $\delta$ = 4.75 (m, 1H, Si-H), 4.66 – 4.57 (m, 6H, Si-H), 4.37 (s, 1H, Cp-H), 4.24 (s, 2H, Cp-H), 0.42 (d, $J$ = 3.3 Hz, 6H, Me), 0.37 (d, $J$ = 3.5 Hz, 6H, Me), 0.36 (d, $J$ = 3.8 Hz, 6H, Me), 0.33 (d, $J$ = 3.9 Hz, 6H, Me), 0.26 (d, $J$ = 3.6 Hz, 6H, Me), 0.24 (d, $J$ = 3.6 Hz, 6H, Me), 0.22 (d, $J$ = 3.6 Hz, 6H, Me) ppm. $^{13}$C{$^1$H} NMR ($CDCl_3$, RT, 176 MHz): $\delta$ = 89.3 (s, Cp-C), 85.4 (s, Cp-C), 84.4 (s, Cp-C), 81.4 (s, Cp-C), 81.1 (s, Cp-C), 78.2 (s, Cp-C), 74.5 (s, Cp-C), 0.0 (s, Me), 0.5 (s, Me), 0.8 (s, Me), 2.1 (s, Me), 2.3 (s, Me), 2.4 (s, Me) ppm. IR (ATR, RT): $\tilde{\nu}$ (cm$^{-1}$) = 2956 ($\nu_{C\text{-}H}$), 2905 ($\nu_{C\text{-}H}$), 2125 ($\nu_{Si\text{-}H}$), 1416, 1382, 1242, 1199, 1117, 1085, 1029, 987, 949, 929, 867, 830, 758, 729. MS (ESI) cald. for $[FeC_{10}DMS_7H_3]^+$: 592.1803. Found: 592.1711. EA: cald. 48.60 (C), 8.84 (H), 0.00 (N), 0.00 (S); found 48.84 (C), 8.79 (H), 0.00 (N), 0.00 (S).

**3b**: 1,2,3,4-tetra(dimethylsilyl)cyclopentadienyl-1,2,3-tri(dimethylsilyl)cyclopentadienyliron(II): red solid 11 mg, 1%. $^1$H NMR ($CDCl_3$, RT, 400 MHz): $\delta$ = 4.69 (m, 4H, Si-H), 4.66 (m, 2H, Si-H), 4.60 (m, 1H, Si-H), 4.54 (s, 2H, Cp-H), 4.41 (s, 1H, Cp-H), 0.45 (d, J = 3.8 Hz, 6H, Me), 0.43 (d, J = 3.2 Hz, 6H, Me), 0.42 (d, J = 3.3 Hz, 6H, Me), 0.38 (d, J = 3.8 Hz, 6H, Me), 0.36 (d, J = 3.9 Hz, 6H, Me), 0.21 – 0.19 (m, 12H, Me) ppm. $^{13}$C{$^1$H} NMR ($CDCl_3$, RT, 176 MHz): $\delta$ = 88.1 (s, Cp-C), 84.1 (s, Cp-C), 82.3 (s, Cp-C), 81.7 (s, Cp-C), 80.9 (s, Cp-C), 80.3 (s, Cp-C), 0.1 (s, Me), -0.2 (s, Me), -0.5 (s, Me), -0.7 (s, Me), -2.4 (s, Me), -2.5 (s, Me) ppm. $^{29}$Si NMR ($CDCl_3$, RT, 80 MHz) $\delta$ = −17.9, −18.1, −21.4, 25.5 ppm. IR (ATR, RT): $\tilde{\nu}$ (cm$^{-1}$) = 2957 (vC-H), 2925 (vC-H), 2856 ($\nu$C-H), 2140 ($\nu$Si-H), 1252, 1197, 1118 ($\delta$C-H), 1077 ($\delta$C-H), 1034 ($\delta$C-H), 951, 878, 827, 800, 799, 760, 737, 698,

660, 634. MS (ESI) cald. for $[FeC_{10}DMS_7H_3]^+$: 592.1803. Found: 592.1711. EA: cald. 48.60 (C), 8.84 (H), 0.00 (N), 0.00 (S); found 48.86 (C), 8.73 (H), 0.00 (N), 0.00 (S).

**Silylation – General Procedure via lithium-bromine exchange.** In a dry Schlenk tube decabromoferrocene (1 g, 1.03 mmol, 1.0 eq.) was placed in anhydrous and degassed *n*-pentane (50 mL) under an argon atmosphere. A solution of *tert*-BuLi (1.6 M in *n*-pentane, 25.8 mL, 41.2 mmol, 40 eq.) was added dropwise at −78 °C and the solution was stirred for 6 h at this temperature. DMSCl (0.690 mL, 61.8 mmol, 60 eq.) was added dropwise and stirred for 6 h at −50 °C. The reaction mixture was slowly warmed up to room temperature overnight. Then, the solvent was removed under reduced pressure and anhydrous *n*-pentane (50 mL) was added again. The resulting red suspension was cooled to (−78 °C) and a solution of *tert*-BuLi (1.6 M in *n*-pentane, 25:8 mL, 41:2 mmol, 40 eq.) was added dropwise at this temperature. The mixture was stirred for 6 h at this temperature. Afterwards, additional DMSCl (0.690 mL, 61.8 mmol, 60 eq.) was added dropwise and the mixture was allowed to warm up to room temperature overnight yielding a pink suspension. All volatile compounds were removed under reduced pressure. Then, saturated $NaHCO_3$ solution was added and extracted with *n*-pentane. The organic layer was dried over $MgSO_4$, filtrated and the organic solvent was removed under reduced pressure to afford a red oil that was pre-purified with column chromatography [$SiO_2$, *n*-pentane]. The crude product was afforded as a red oil and was further purified by HPLC [RP-18, MeOH/$H_2O$ (98:2) then MeOH]. Several highly silylated but still brominated ferrocenes could be isolated.

**1**: Bis(1-bromo-2,3,4,5-tetra(dimethylsilyl)cyclopentadienyl)iron(II): pink solid (130 mg, 16%). $^1$H NMR ($CDCl_3$, RT, 400 MHz): $\delta$ = 4.72 (hept, $J$ = 3.3, 2.8 Hz, 2H, Si-H), 4.64 (hept, $J$ = 4.0 Hz, 2H, Si-H), 0.76 (d, $J$ = 4.0 Hz, 6H, Me), 0.41 (d, $J$ = 4.0 Hz, 6H, Me), 0.39 (d, $J$ = 4.0 Hz, 6H, Me), 0.22 (d, $J$ = 3.9 Hz, 6H, Me) ppm. $^{13}$C{$^1$H} NMR ($CDCl_3$, RT, 176 MHz): $\delta$ = 99.4 (s, Cp-C), 87.7 (s, Cp-C), 85.0 (s, Cp-C), 0.5 (s, Me), 0.2 (s, Me), -0.0 (s, Me), -1.2 (s, Me) ppm. $^{29}$Si NMR ($CDCl_3$, RT, 80 MHz) $\delta$ = -17.4, -18.4 ppm. MS (EI) cald for $[FeC_{10}DMS_8Br_2]^+$: 808.0231. Found: 808.0328.

**2**: 1,2,3,4,5-penta(dimethylsilyl)cyclopentadienyl-1-bromo-2,3,4,5-tetra(dimethylsilyl)cyclopentadienyliron(II): purple solid (210 mg, 26%). $^1$H NMR ($CDCl_3$, RT, 400 MHz): $\delta$ = 4.74 (hept, $J$ = 3.9 Hz, 2H, Si-H), 4.60 (hept, $J$ = 3.7 Hz, 5H, Si-H), 4.51 (hept, $J$ = 3.8 Hz, 2H, Si-H), 0.39 (m, 60H, Me) ppm. $^{13}$C{$^1$H} NMR ($CDCl_3$, RT, 176 MHz): $\delta$ = 97.8 (s, Cp-C), 93.8 (s, Cp-C), 86.8 (s, Cp-C), 84.6 (s, Cp-C), 0.7 (s, Me), 0.4 (s, Me), -0.5 (s, Me) ppm. MS (EI) cald for $[FeC_{10}DMS_9Br]^+$: 788.1364. Found: 788.1330.

In a dry 50 mL Schlenk tube the mixture of partially brominated silylferrocenes (430 mg.) was placed in anhydrous and degassed tetrahydrofuran (5 mL) under an argon atmosphere. A solution of *tert*-BuLi (1.6 M in *n*-pentane, 25.8 mL, 41.2 mmol) was added dropwise at −78 °C. The dark red solution warmed up to at −20 °C over a period of 1 h. DMSCl (0.690 mL, 61.8 mmol) was added dropwise and the reaction mixture was slowly warmed up to room temperature overnight. After heating at 50 °C for 1 h, all volatile compounds were removed under reduced pressure. Then, saturated $NaHCO_3$ solution was added and extracted with *n*-pentane. The organic layer was dried over $MgSO_4$, filtrated and the organic solvent was removed under reduced pressure to afford a pink oil that was prepurified with column chromatography [$SiO_2$, *n*-pentane]. The crude product was afforded as a pink oil which was first recrystallized from THF or *n*-pentane (to yield $[FeC_{10}DMS_{10}]$ (**3**) as pink solid) and subsequently purified by HPLC [RP-18, 9:1 MeOH(98%) and THF]. Several highly silylated ferrocenes could be isolated.

**6**: Bis(1,2,3,4,5-penta(dimethylsilyl)cyclopentadienyl)iron(II): purple solid, 10 mg, 1%. $^1$H NMR ($CDCl_3$, RT, 400 MHz): $\delta$ = 4.64 (hept, $J$ = 4.0 Hz, 10H, Si-H), 0.76 (d, $J$ = 3.6 Hz, 30H, Me), 0.09 (d, $J$ = 3.7 Hz, 30H, Me) ppm. $^{13}$C{$^1$H} NMR ($CDCl_3$, RT, 176 MHz): δ = 93.21, 2.41, −0.18 ppm. $^{29}$Si NMR ($CDCl_3$, RT, 80 MHz) $\delta$ = -17.9 ppm. IR (ATR, RT): $\tilde{\nu}$ ($cm^{-1}$) = 2976 ($\nu_{C\text{-}H}$), 2908 ($\nu_{C\text{-}H}$), 2155 ($\nu_{Si\text{-}H}$), 1242, 1222, 914, 880, 831, 757, 697, 666. MS (ESI) cald for $[FeC_{10}DMS_{10}]^+$: 766.2520. Found: 766.2530. EA: cald. 46.94 (C), 9.19 (H), 0.00 (N), 0.00 (S); found 46.86 (C), 8.75 (H), 0.00 (N), 0.00 (S).

**5**: 1,2,3,4,5-penta(dimethylsilyl)cyclopentadienyl-1,2,3,4-tetra(dimethylsilyl)cyclopentadienyliron(II): purple solid, 41 mg, 6%. $^{1}$H NMR ($CDCl_3$, RT, 400 MHz): $\delta$ = 4.74 (hept, $J$ = 3.5 Hz, 2H, Si-H), 4.67 (hept, $J$ = 3.8 Hz, 5H, Si-H), 4.63 – 4.60 (m, 2H, Si-H), 4.59 (s, 1H, Cp-H), 0.39 (m, 42H, Me), 0.35 (d, $J$ = 3.7 Hz, 6H, Me), 0.16 (d, $J$ = 3.7 Hz, 6H, Me) ppm. $^{13}$C{$^{1}$H} NMR ($CDCl_3$, RT, 176 MHz): $\delta$ = 90.8 (s, Cp-C), 87.8 (s, Cp-C), 86.4 (s, Cp-C), 83.6 (s, Cp-C), 0.9 (s, Me), 0.8 (s, Me), 0.4 (s, Me), 0.1 (s, Me), -1.01 (s, Me) ppm. $^{29}$Si NMR ($CDCl_3$, RT, 80 MHz) $\delta$ = -17.4, -18.8 ppm. IR (ATR, RT): $\tilde{\nu}$ ($cm^{-1}$) = 2959 ($\nu_{C\text{-}H}$), 2906 ($\nu_{C\text{-}H}$), 2147 ($\nu_{Si\text{-}H}$), 1243, 1229, 1194, 1106 ($\delta_{C\text{-}H}$), 1069 ($\delta_{C\text{-}H}$), 1036 ($\delta_{C\text{-}H}$), 948, 870, 829, 757, 698, 758, 698, 663. MS (ESI) cald for $[FeC_{10}DMS_9H]^+$: 708.2281. Found: 708.2238. EA: cald. 47.41 (C), 9.09 (H), 0.00 (N), 0.00 (S); found 47.21 (C), 8.52 (H), 0.01 (N), 0.00 (S).

**Silylation of 1,1'-dimethyl ferrocene.** Mercury(II) butyrate (28.81 g, 76.7 mmol, 8,2 eq.) and 1,2-dichloroethane (200 mL) were placed in a 500 mL round bottom flask. 1,1'-dimethyl ferrocene (2 g, 9.34 mmol, 1.0 Eq.) was added and the suspension was stirred under reflux for 18 h. The orange solution allowed to cool down and filtered off, subsequently. Then, the solvent was removed under reduced pressure to afford a orange solid. Without further purification, deionized water (250 mL), bromine (30.00 g, 166.67 mmol, 17.7 eq.) and potassium bromide (34.00 g, 285.71 mmol, 30.6 eq.) were added. The suspension was stirred for four days at room temperature. Afterwards, the mixture was filtered off and the residue was washed with deionized water and methanol. The product, $[FeC_{10}Me_2Br_8]$, was extracted in DCM. The solvent was removed under reduced pressure and washed with (a few milliliters of) dichloromethane to yield a yellow solid (4.2 g, 53%).

$[FeC_{10}Me_2Br_8]$ (**7**): $^{1}$H NMR ($CDCl_3$, RT, 700 MHz): $\delta$ = 1.98 (s, Me-H) ppm. $^{13}$C{$^{1}$H} NMR ($CDCl_3$, RT, 176 MHz): $\delta$ = 85.3 (s, Cp-C), 84.1 (s, Cp-C), 82.3 (s, Cp-C), 9,8 (s, Me-C) ppm. IR (ATR, RT): $\tilde{\nu}$ ($cm^{-1}$) = 2964, 2874, 1520, 1497, 1370, 1345, 1262, 1218, 1093, 896, 754, 722, 589. MS (EI) cald for $[FeC_{10}Me_2Br_8]^+$: 845.3204. Found: 845.3196. EA: cald. 17.05 (C), 0.72 (H), 0.00 (N), 0.00 (S); found 16.91 (C), 0.43 (H), 0.01 (N), 0.00 (S).

In a dry 50 mL pressure tube magnesium (0.42 g, 18.26 mmol, 11 eq.) was placed in anhydrous and degassed THF (10 mL) under an argon atmosphere. Then DMSCl (5 mL, 45.03 mmol, 27 eq.) and $[FeC_{10}Me_2Br_8]$ (1.4 g, 1.65 mmol, 1.0 eq.) were suspended in anhydrous and degassed THF (15 mL) were added subsequently dropwise and the reaction mixture was stirred for 16 h at room temperature. Then, the solvent was evaporated under reduced pressure by using a cooling trap. The compound was extracted in anhydrous *n*-pentane and filtered off. The solvent was removed under reduced pressure to yield a pink oil which was washed with methanol. The residue was dried at high vacuum to afford the product as pink solid (0.99 g, 88%).

$[FeC_{10}Me_2DMS_8]$ (**8**): $^{1}$H NMR ($CDCl_3$, RT, 700 MHz): $\delta$ = 4.64 (m, Si-H, 2H), 4.58 (m, Si-H, 2H), 2.14 (s, $Me^{Cp}$, 3H), 0.53 (d, $J$ = 3.8 Hz, 6H), 0.36 (d, $J$ = 3.8 Hz, 6H), 0.33 (d, J = 3.8 Hz, 6H), 0.14 (d, $J$ = 3.7 Hz, 1H) ppm. $^{13}$C{$^{1}$H} NMR ($CDCl_3$, RT, 176 MHz): $\delta$ = 86.4 (Cp-C), 82.5 (Cp-C), 16.7 ($Me^{Cp}$), 0.5 (DMS), 0.1 (DMS), −0.6 (DMS), −0.8 (DMS) ppm. $^{29}$Si NMR ($CDCl_3$, RT, 80 MHz) $\delta$ = −19.3 ppm. IR (ATR, RT): $\tilde{\nu}$ ($cm^{-1}$) = 2957, 2903, 2153, 1384, 1334, 1245, 1220, 1022, 877, 827, 759, 676, 643. MS (EI) cald for $[FeC_{10}Me_2Br_8]^+$: 678.2355. Found: 678.2460. EA: cald. 49.51 (C), 9.20 (H), 0.00 (N), 0.00 (S); found 49.12 (C), 9.48 (H), 0.02 (N), 0.00 (S).

# 3 Crystal Structure Determination

X-Ray data were collected on a BRUKER D8 Venture system. Data were collected at 100(2) K using graphite-monochromated Mo $K_\alpha$ ($\lambda_\alpha$ = 0.71073 Å) or Cu $K_\alpha$ ($\lambda$ = 1.54178) radiation. The strategy for the data collection was evaluated by using the Smart software. The data were collected by the standard "ψ-ω scan techniques" and were scaled and reduced using Saint+software. The structures were solved by using Olex2,[8] the structure was solved with the XT[9] structure solution program using Intrinsic Phasing and refined with the XL refinement package[10,11] using Least Squares minimization. If it is noted, bond length and angles were measured with Diamond Crystal and Molecular Structure Visualization Version 4.6.2.[12] Drawings were generated with POV-Ray.[13] Deposition numbers CCDC 2248053 (**1**), 2248054 (**2**), 2248060 (**3a**), 2248059 (**3b**), 2248057 (**4a**), 2248058 (**4b**), 2248056 (**5**), 2248055 (**6**) contain the supplementary crystallographic data for this paper. These data are provided free of charge by the joint Cambridge Crystallographic Data Centre and Fachinformationszentrum Karlsruhe Access Structures service www.ccdc.cam.ac.uk/structures.

Table S2. Crystal data.

| **Compound** | **$FeC_{10}(DMS)_9Br$ (2)** | **$Fe(C_5(DMS)_4Br)_2$ (1)** |
|---|---|---|
| **Empirical formula** | $C_{28}H_{63}BrFeSi_9$ | $C_{26}H_{56}Br_2FeSi_8$ |
| **Formula weight** | 788.35 | 809.09 |
| **Temperature/K** | 100.0 | 100 |
| **Crystal system** | orthorhombic | tetragonal |
| **Space group** | Pnma | $P4_2/n$ |
| **a/Å** | 17.7129(9) | 36.0111(3) |
| **b/Å** | 18.7916(7) | 36.0111(3) |
| **c/Å** | 12.3172(6) | 12.1108(2) |
| **α/°** | 90 | 90 |
| **β/°** | 90 | 90 |
| **γ/°** | 90 | 90 |
| **Volume/Å³** | 4099.8(3) | 15705.3(4) |
| **Z** | 4 | 16 |
| **$\rho_{calc}$/g·cm³** | 1.277 | 1.369 |
| **μ/mm⁻¹** | 1.624 | 7.919 |
| **F(000)** | 1672.0 | 6720.0 |
| **Crystal size/mm³** | 0.22 × 0.22 × 0.18 | 0.23 × 0.23 × 0.22 |
| **Crystal shape** | Block | Block |
| **Radiation** | MoKα (λ = 0.71073) | CuKα (λ = 1.54178) |
| **2Θ range for data collection/°** | 4.028 to 56.602 | 5.488 to 136.552 |
| **Index ranges** | $-23 \le h \le 23$, $-25 \le k \le 24$, $-16 \le l \le 16$ | $-43 \le h \le 43$, $-42 \le k \le 43$, $-13 \le l \le 14$ |
| **Reflections collected** | 72426 | 83076 |
| **Independent reflections** | 5235 [$R_{int}$ = 0.0502, $R_{sigma}$ = 0.0194] | 14394 [$R_{int}$ = 0.0678, $R_{sigma}$ = 0.0438] |
| **Data/restrains/parameters** | 5235/0/238 | 14394/0/700 |
| **Goodness-of-fit on $F^2$** | 1.050 | 1.035 |
| **Final R indexes [I>=2σ(I)]** | $R_1$ = 0.0297, $wR_2$ = 0.0792 | $R_1$ = 0.0473, $wR_2$ = 0.1249 |
| **Final R indexes [all data]** | $R_1$ = 0.0357, $wR_2$ = 0.0823 | $R_1$ = 0.0536, $wR_2$ = 0.1295 |
| **Largest diff. peak/hole / e·Å³** | 0.53/−0.35 | 2.16/-1.39 |

Table S3. Crystal data.

| **Compound** | **$FeC_{10}(DMS)_{10}$ (6)** | **$FeC_{10}(DMS)_9H$ (5)** |
|---|---|---|
| **Empirical formula** | $C_{30}H_{70}FeSi_{10}$ | $C_{28}H_{64}FeSi_9$ |
| **Formula weight** | 767.61 | 709.45 |
| **Temperature/K** | 100.00 | 100 |
| **Crystal system** | monoclinic | triclinic |
| **Space group** | $P2_1/n$ | P-1 |
| **a/Å** | 11.9543(6) | 11.9336(7) |
| **b/Å** | 13.4426(7) | 18.9321(12) |
| **c/Å** | 13.3587(6) | 20.4215(13) |
| **α/°** | 90 | 63.840(2) |
| **β/°** | 93.029(2) | 77.549(2) |
| **γ/°** | 90 | 88.306(2) |
| **Volume/Å$^3$** | 2143.70(18) | 4032.5(4) |
| **Z** | 2 | 4 |
| **$\rho_{calc}$g/cm$^3$** | 1.189 | 1.169 |
| **μ/mm$^{-1}$** | 0.651 | 0.659 |
| **F(000)** | 832.0 | 1536.0 |
| **Crystal size/mm$^3$** | 0.11 × 0.08 × 0.07 | 0.1 × 0.1 × 0.1 |
| **Crystal shape** | block | block |
| **Radiation** | MoKα (λ = 0.71073) | MoKα (λ = 0.71073) |
| **2Θ range for data collection/°** | 4.456 to 52.736 | 3.982 to 56.564 |
| **Index ranges** | $-14 \le h \le 14$, $-16 \le k \le 16$, $-16 \le l \le 16$ | $-15 \le h \le 15$, $-25 \le k \le 25$, $-27 \le l \le 27$ |
| **Reflections collected** | 60684 | 133719 |
| **Independent reflections** | 4386 [$R_{int}$ = 0.0765, $R_{sigma}$ = 0.0284] | 19977 [$R_{int}$ = 0.0519, $R_{sigma}$ = 0.0320] |
| **Data/restraints/parameters** | 4386/0/255 | 19977/0/956 |
| **Goodness-of-fit on F$^2$** | 1.017 | 1.071 |
| **Final R indexes [I>=2σ (I)]** | $R_1$ = 0.0272, $wR_2$ = 0.0623 | $R_1$ = 0.0423, $wR_2$ = 0.1001 |
| **Final R indexes [all data]** | $R_1$ = 0.0339, $wR_2$ = 0.0656 | $R_1$ = 0.0534, $wR_2$ = 0.1055 |
| **Largest diff. peak/hole / e Å$^{-3}$** | 0.33/-0.23 | 0.75/-0.48 |

| Compound | $Fe(C_5(DMS)_5)(1,2,3\text{-}C_5(DMS)_3H_2)$ (4a) | $Fe(C_5(DMS)_4H)_2$ (4b) |
|---|---|---|
| **Empirical formula** | $C_{26}H_{58}FeSi_8$ | $C_{26}H_{58}FeSi_8$ |
| **Formula weight** | 651.29 | 651.29 |
| **Temperature/K** | 100.0 | 100.0 |
| **Crystal system** | monoclinic | monoclinic |
| **Space group** | Cc | $P2_1/n$ |
| **a/Å** | 18.8023(14) | 19.7412(7) |
| **b/Å** | 16.3214(13) | 20.9752(7) |
| **c/Å** | 11.9698(9) | 19.7446(7) |
| **α/°** | 90 | 90 |
| **β/°** | 94.187(3) | 112.4200(10) |
| **γ/°** | 90 | 90 |
| **Volume/Å$^3$** | 3663.5(5) | 7557.8(5) |
| **Z** | 4 | 8 |
| **$\rho_{calc}$g/cm$^3$** | 1.181 | 1.145 |
| **μ/mm$^{-1}$** | 0.688 | 0.667 |
| **F(000)** | 1408.0 | 2816.0 |
| **Crystal size/mm$^3$** | 0.18 × 0.14 × 0.12 | 0.27 × 0.23 × 0.11 |
| **Crystal shape** | block | block |
| **Radiation** | MoKα (λ = 0.71073) | MoKα (λ = 0.71073) |
| **2Θ range for data collection/°** | 4.344 to 50.754 | 3.71 to 50.804 |
| **Index ranges** | $-22 \le h \le 22$, $-19 \le k \le 19$, $-14 \le l \le 14$ | $-23 \le h \le 23$, $-19 \le k \le 25$, $-23 \le l \le 23$ |
| **Reflections collected** | 25907 | 85294 |
| **Independent reflections** | 6673 [$R_{int}$ = 0.0726, $R_{sigma}$ = 0.0641] | 13876 [$R_{int}$ = 0.0833, $R_{sigma}$ = 0.0585] |
| **Data/restraints/parameters** | 6673/2/332 | 13876/0/663 |
| **Goodness-of-fit on F$^2$** | 0.813 | 0.969 |
| **Final R indexes [I>=2σ (I)]** | $R_1$ = 0.0397, $wR_2$ = 0.1088 | $R_1$ = 0.0457, $wR_2$ = 0.1323 |
| **Final R indexes [all data]** | $R_1$ = 0.0450, $wR_2$ = 0.1154 | $R_1$ = 0.0778, $wR_2$ = 0.1580 |
| **Largest diff. peak/hole / e Å$^{-3}$** | 0.49/-0.36 | 0.52/-0.47 |

| Compound | $Fe(C_5(DMS)_4H)(1,2,4\text{-}C_5(DMS)_3H_2)$ (3a) | $Fe(C_5(DMS)_4H)(1,2,3\text{-}C_5(DMS)_3H_2)$ (3b) |
|---|---|---|
| **Empirical formula** | $C_{24}H_{52}FeSi_7$ | $C_{24}H_{52}FeSi_7$ |
| **Formula weight** | 593.13 | 593.13 |
| **Temperature/K** | 100.0 | 159.0 |
| **Crystal system** | triclinic | triclinic |
| **Space group** | P-1 | P-1 |
| **a/Å** | 9.6168(3) | 11.1775(6) |
| **b/Å** | 10.8650(4) | 12.2628(6) |
| **c/Å** | 17.6366(7) | 13.4623(7) |
| **α/°** | 78.884(2) | 79.414(2) |
| **β/°** | 81.1830(10) | 68.618(2) |
| **γ/°** | 65.9980(10) | 80.572(2) |
| **Volume/Å$^3$** | 1646.09(10) | 1679.52(15) |
| **Z** | 2 | 2 |
| **$\rho_{calc}$g/cm$^3$** | 1.197 | 1.173 |
| **μ/mm$^{-1}$** | 0.725 | 0.711 |
| **F(000)** | 640.0 | 640.0 |
| **Crystal size/mm$^3$** | 0.31 × 0.3 × 0.25 | 0.25 × 0.25 × 0.23 |
| **Crystal shape** | block | block |
| **Radiation** | MoKα (λ = 0.71073) | MoKα (λ = 0.71073) |
| **2Θ range for data collection/°** | 4.148 to 56.628 | 4.802 to 56.61 |
| **Index ranges** | $-12 \le h \le 12$, $-14 \le k \le 14$, $-23 \le l \le 23$ | $-14 \le h \le 14$, $-16 \le k \le 16$, $-17 \le l \le 17$ |
| **Reflections collected** | 106271 | 136233 |
| **Independent reflections** | 8170 [$R_{int}$ = 0.0555, $R_{sigma}$ = 0.0215] | 8332 [$R_{int}$ = 0.0577, $R_{sigma}$ = 0.0206] |
| **Data/restraints/parameters** | 8170/0/303 | 8332/0/303 |
| **Goodness-of-fit on F$^2$** | 1.023 | 1.041 |
| **Final R indexes [I>=2σ (I)]** | $R_1$ = 0.0332, $wR_2$ = 0.0871 | $R_1$ = 0.0330, $wR_2$ = 0.0873 |
| **Final R indexes [all data]** | $R_1$ = 0.0396, $wR_2$ = 0.0901 | $R_1$ = 0.0392, $wR_2$ = 0.0911 |
| **Largest diff. peak/hole / e Å$^{-3}$** | 0.65/-0.68 | 0.77/-0.65 |

| **Compound** | **$FeC_{10}Me_2DMS_8$ (8)** |
|---|---|
| **Empirical formula** | $C_{28}H_{62}FeSi_8$ |
| **Formula weight** | 679.34 |
| **Temperature/K** | 102.0 |
| **Crystal system** | orthorhombic |
| **Space group** | $P2_12_12$ |
| **a/Å** | 17.4074(6) |
| **b/Å** | 35.0636(12) |
| **c/Å** | 12.7379(4) |
| **α/°** | 90 |
| **β/°** | 90 |
| **γ/°** | 90 |
| **Volume/Å$^3$** | 7774.8(4) |
| **Z** | 8 |
| **$\rho_{calc}$g/cm$^3$** | 1.161 |
| **μ/mm$^{-1}$** | 0.651 |
| **F(000)** | 2944.0 |
| **Crystal size/mm$^3$** | 0.53 × 0.37 × 0.29 |
| **Crystal shape** | block |
| **Radiation** | MoKα (λ = 0.71073) |
| **2Θ range for data collection/°** | 3.952 to 56.664 |
| **Index ranges** | $-23 \leq h \leq 23$, $-46 \leq k \leq 46$, $-14 \leq l \leq 16$ |
| **Reflections collected** | 168102 |
| **Independent reflections** | 19338 [$R_{int}$ = 0.0397, $R_{sigma}$ = 0.0245] |
| **Data/restraints/parameters** | 19338/0/731 |
| **Goodness-of-fit on F$^2$** | 1.048 |
| **Final R indexes [I>=2σ (I)]** | $R_1$ = 0.0440, $wR_2$ = 0.1201 |
| **Final R indexes [all data]** | $R_1$ = 0.0459, $wR_2$ = 0.1214 |
| **Largest diff. peak/hole / e Å$^{-3}$** | 1.43/-0.70 |

# 4 Spectra

## 5.1 NMR spectra of brominated silylferrocenes

1,2,3,4,5-penta(dimethylsilyl)cyclopentadienyl-1-bromo-2,3,4,5-tetra(dimethylsilyl)-cyclopentadienyliron(II):

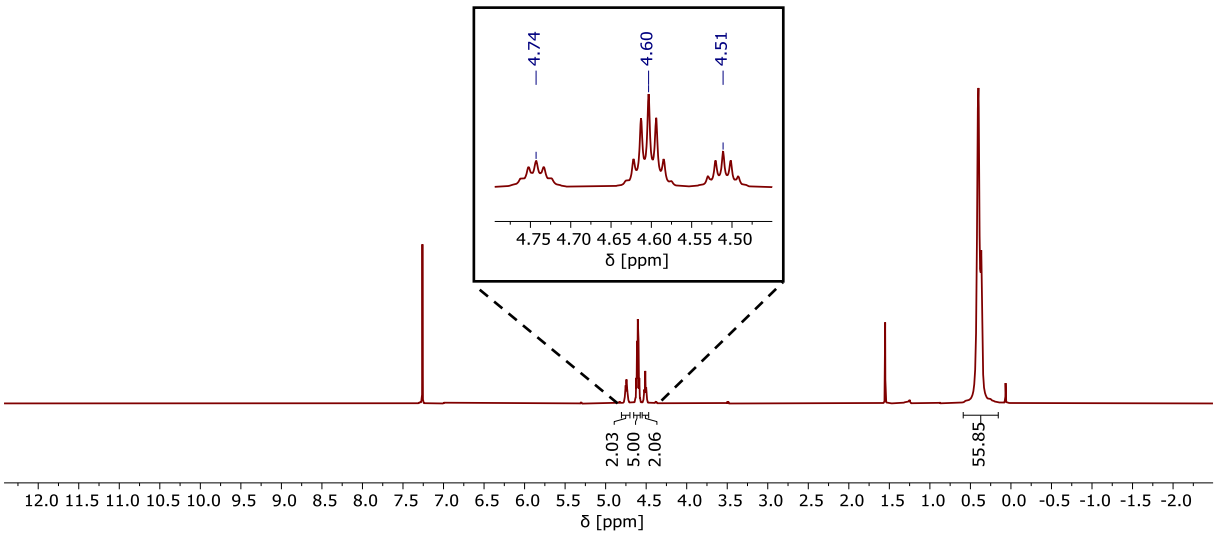


Figure S1. $^{1}H$ NMR spectrum ($CDCl_3$, RT, 400 MHz).

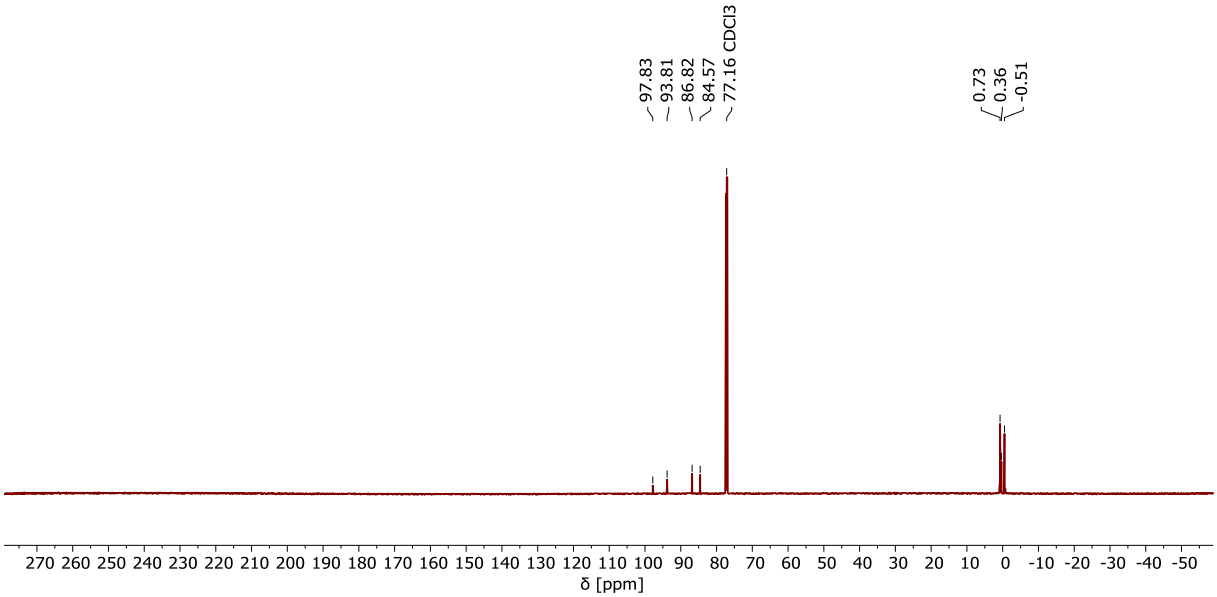


Figure S2. $^{13}C\{^{1}H\}$ NMR spectrum ($CDCl_3$, RT, 176 MHz).

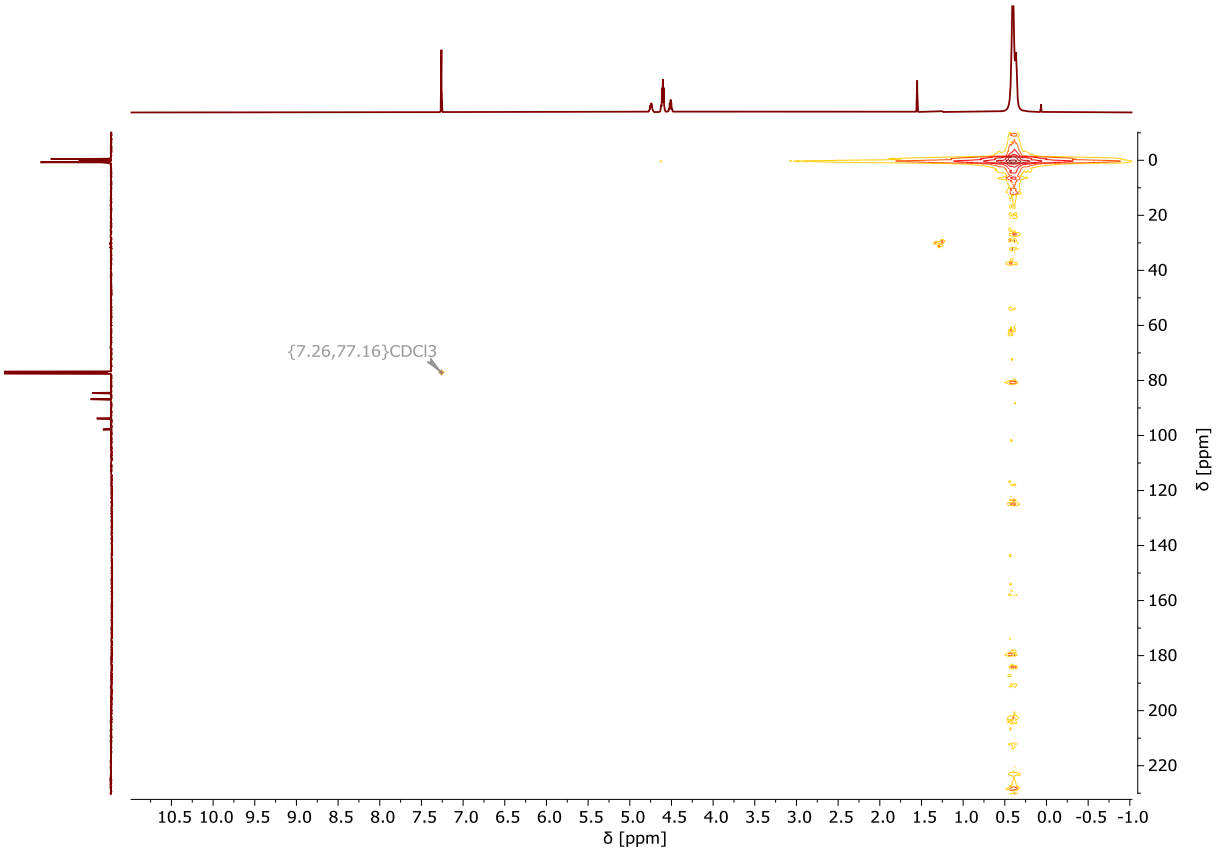


Figure S3. $^{1}H,^{13}C$ HMQC NMR spectrum.

## Bis(1-bromo-2,3,4,5-tetra(dimethylsilyl)cyclopentadienyl)iron(II):

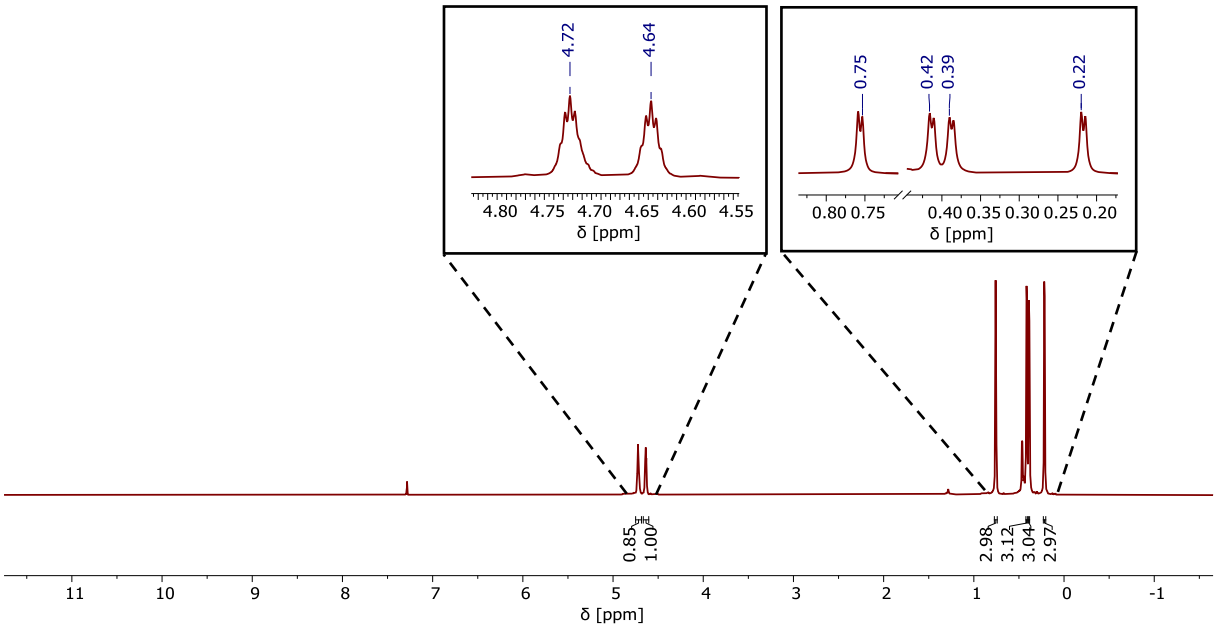


Figure S4. $^{1}H$ NMR spectrum ($CDCl_3$, RT, 400 MHz).

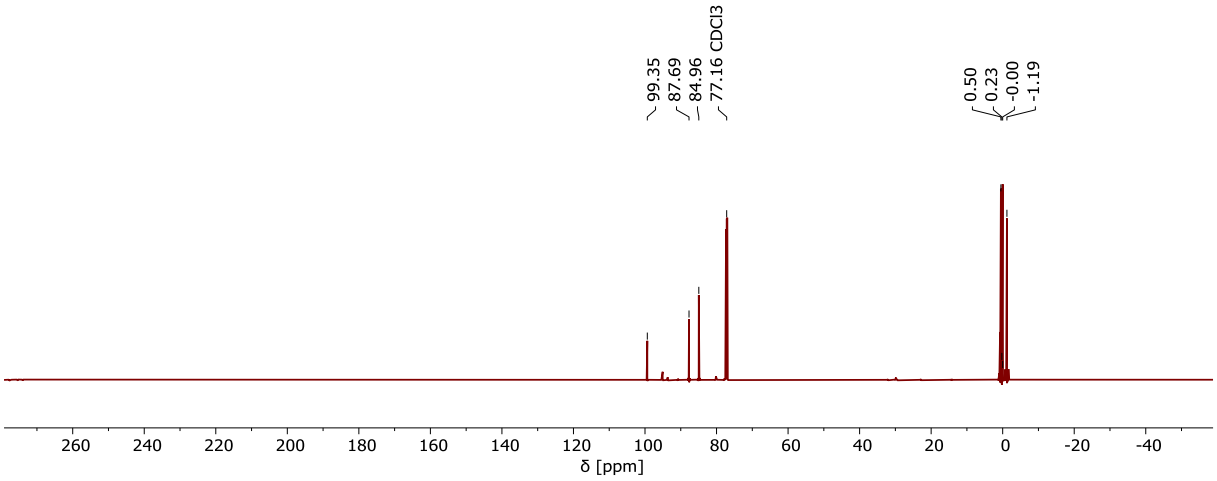


Figure S5. $^{13}C\{^{1}H\}$ NMR spectrum ($CDCl_3$, RT, 176 MHz).

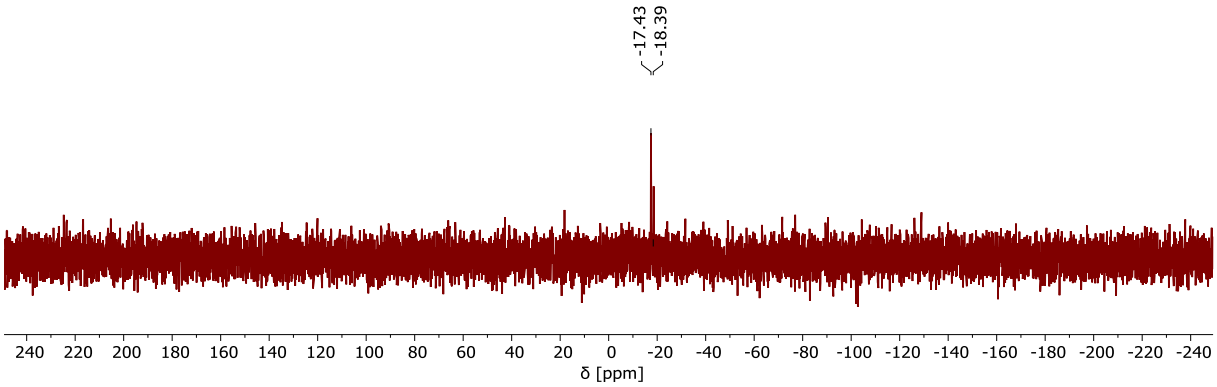


Figure S6. $^{29}Si$ DEPT spectrum ($CDCl_3$, RT, 80 MHz).

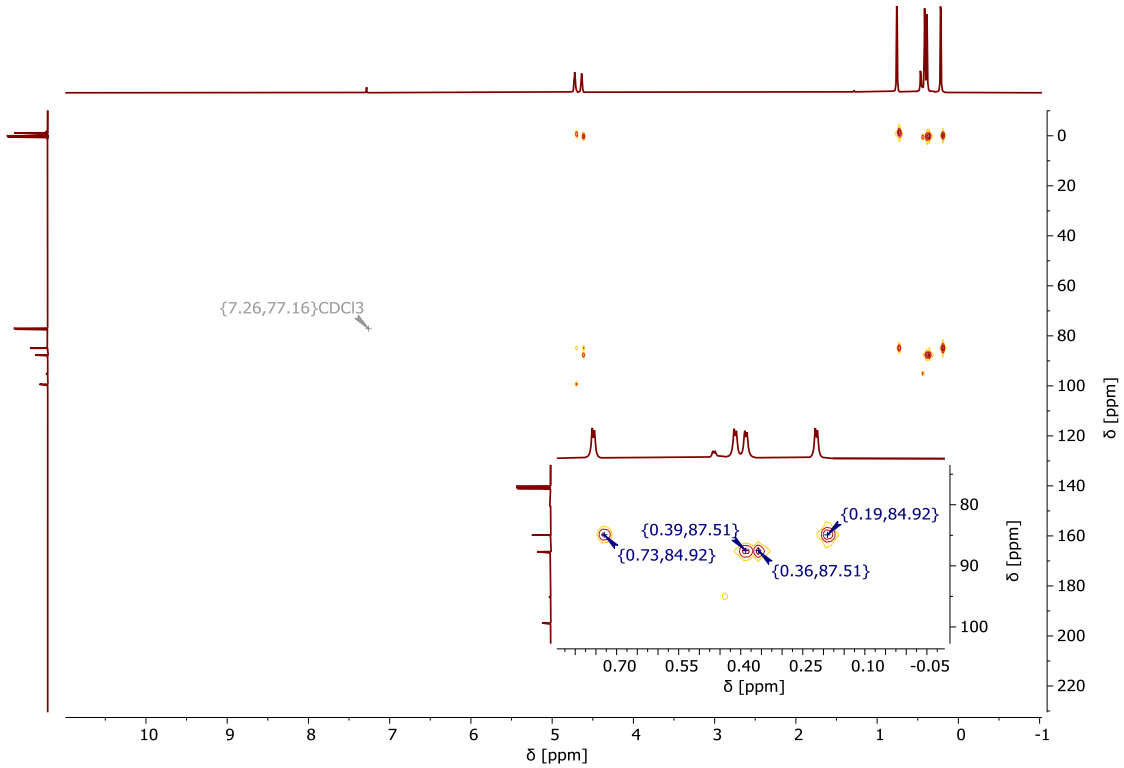


Figure S7. $^{1}H,^{13}C$ HMBC NMR spectrum.

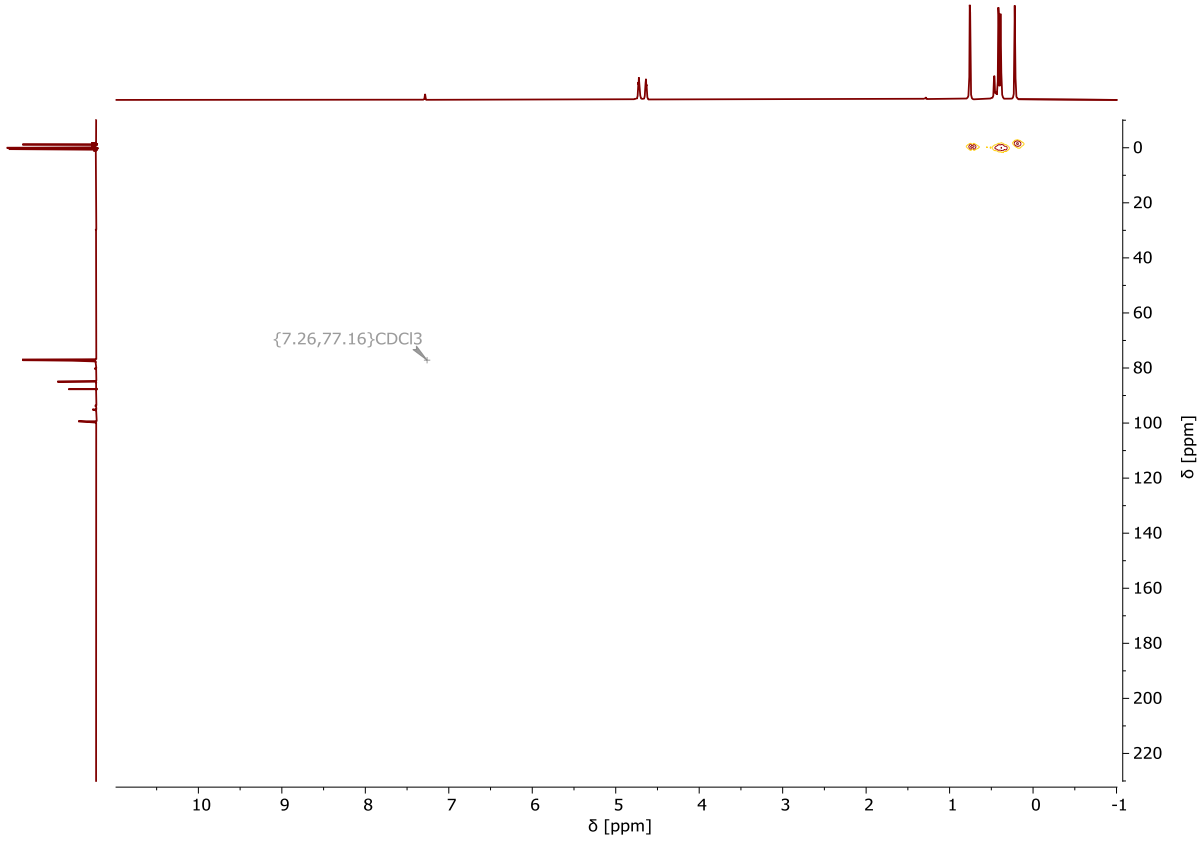


Figure S8. $^{1}H,^{13}C$ HMQC NMR spectrum.

## 5.2 NMR spectra of polysilylated ferrocenes

Bis(1,2,3,4,5-penta(dimethylsilyl)cyclopentadienyl)iron(II):

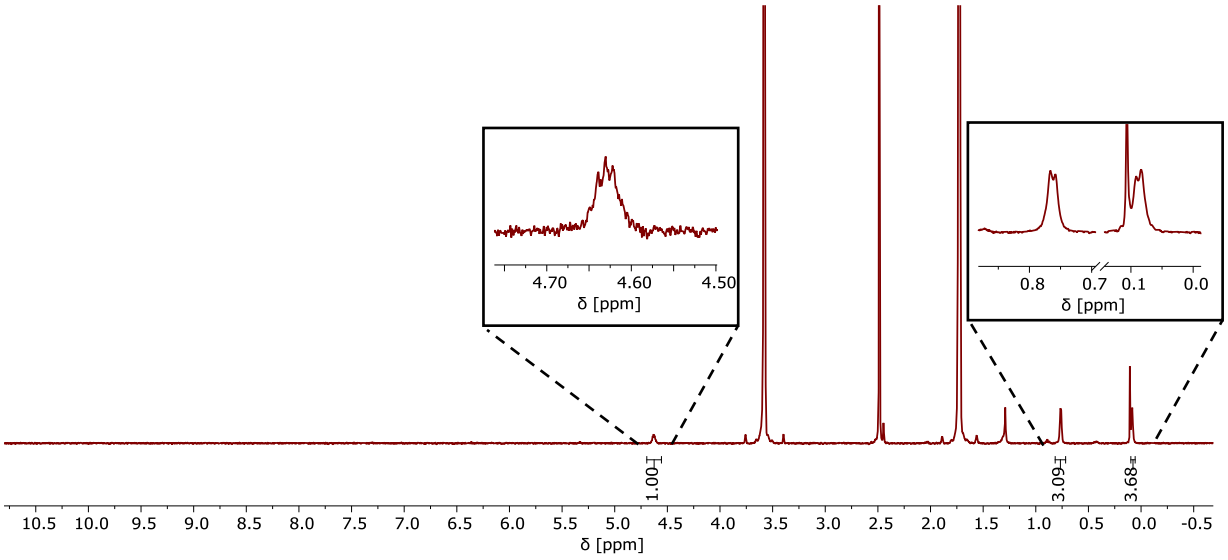


Figure S9. $^{1}H$ NMR spectrum (THF-$d_8$, RT, 400 MHz).

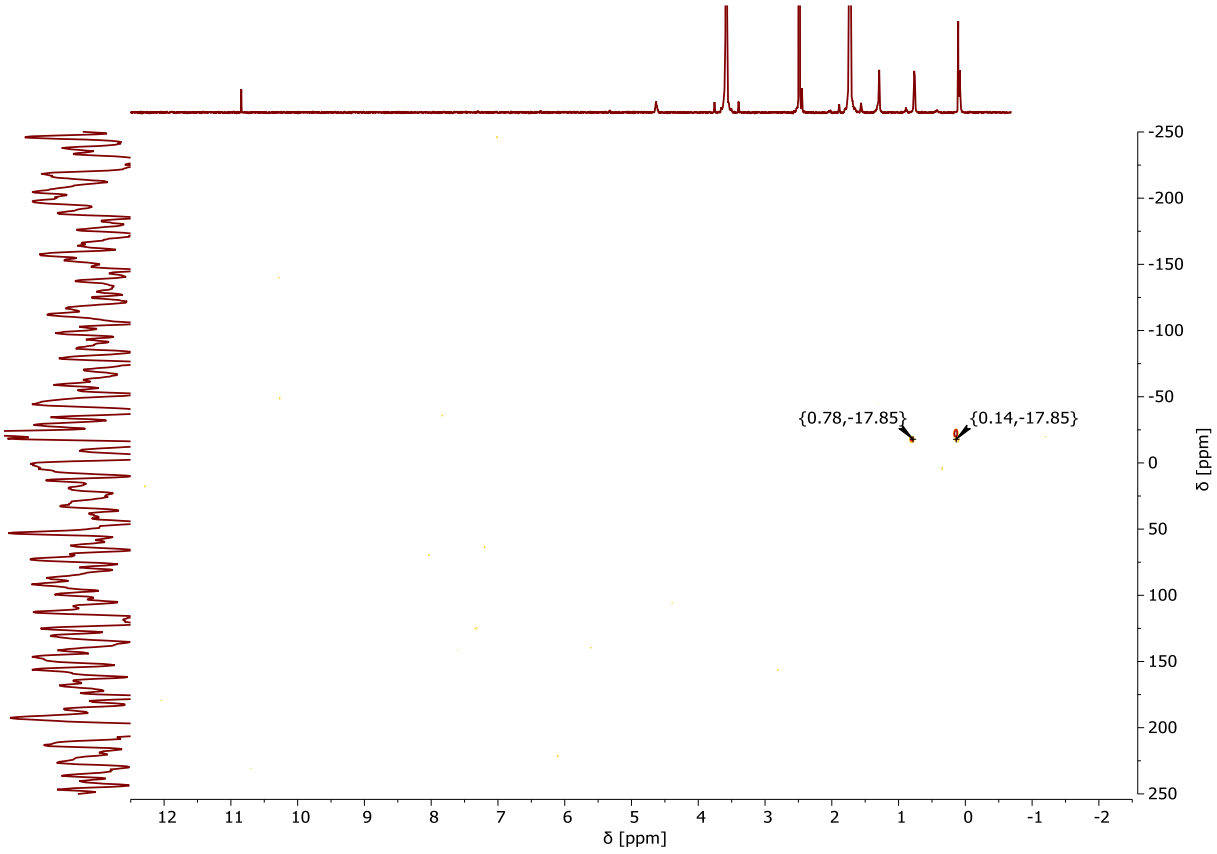


Figure S10. $^{1}H,^{29}Si$ HMBC NMR spectrum.

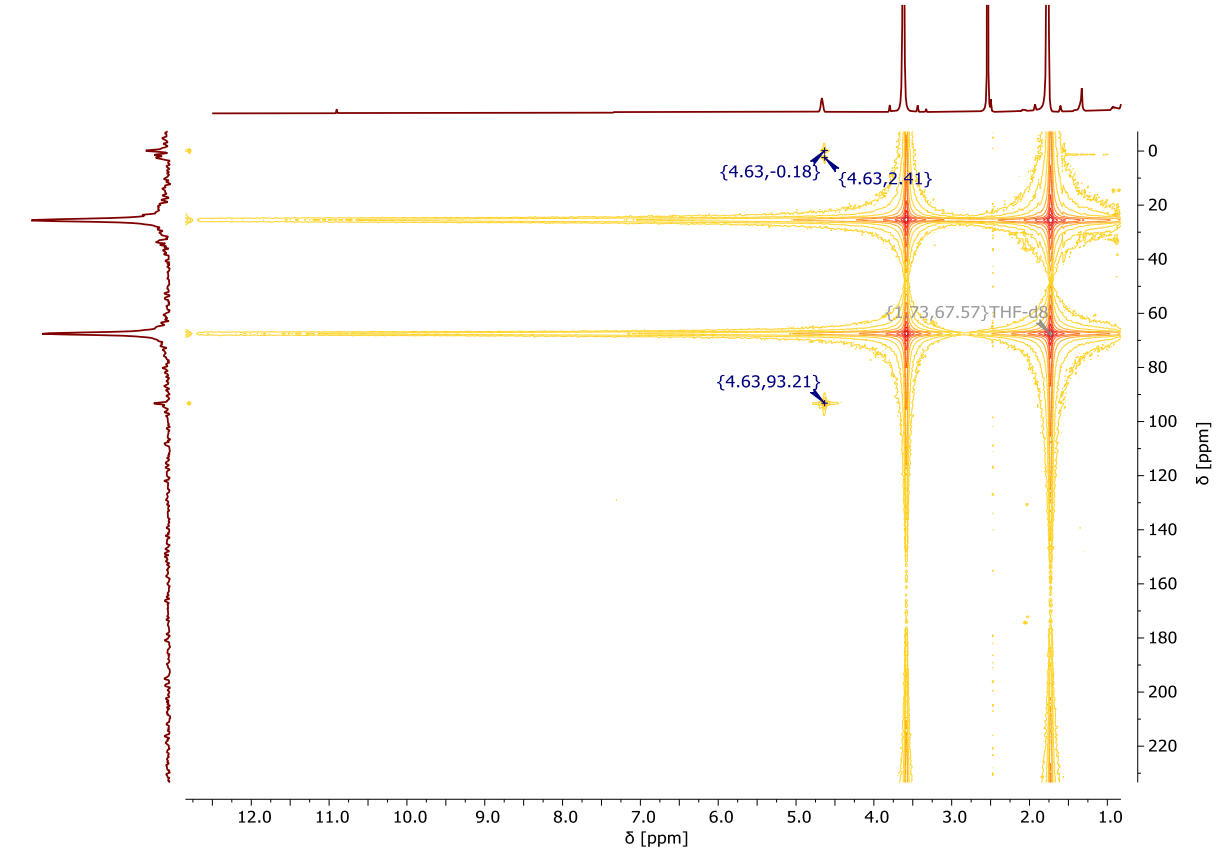


Figure S11. $^{1}H,^{13}C$ HMBC NMR spectrum.

1,2,3,4,5-penta(dimethylsilyl)cyclopentadienyl-1,2,3,4-tetra(dimethylsilyl)cyclopentadienyl-iron(II):

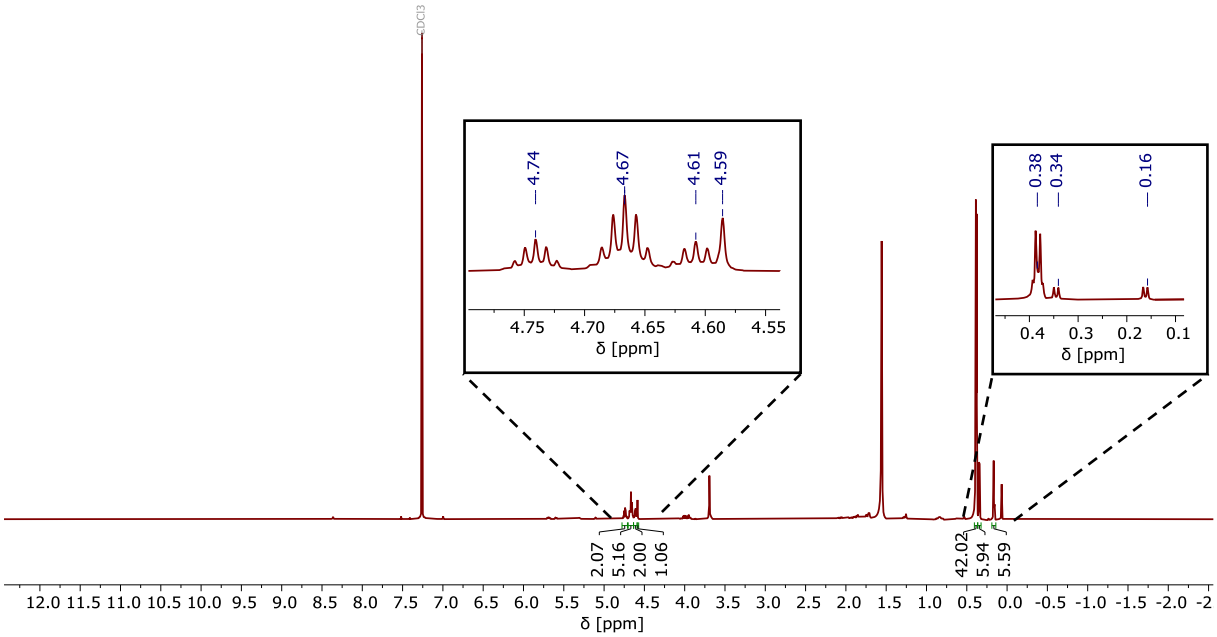


Figure S12. $^{1}H$ NMR spectrum (400 MHz, $CDCl_3$, RT).

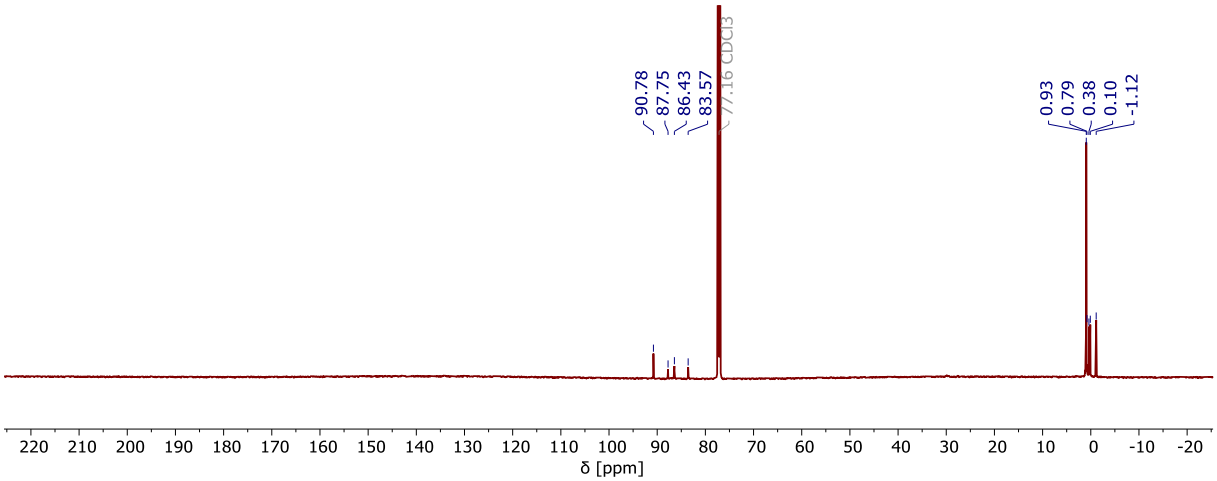


Figure 13. $^{13}C$ NMR spectrum (176 MHz, $CDCl_3$, RT).

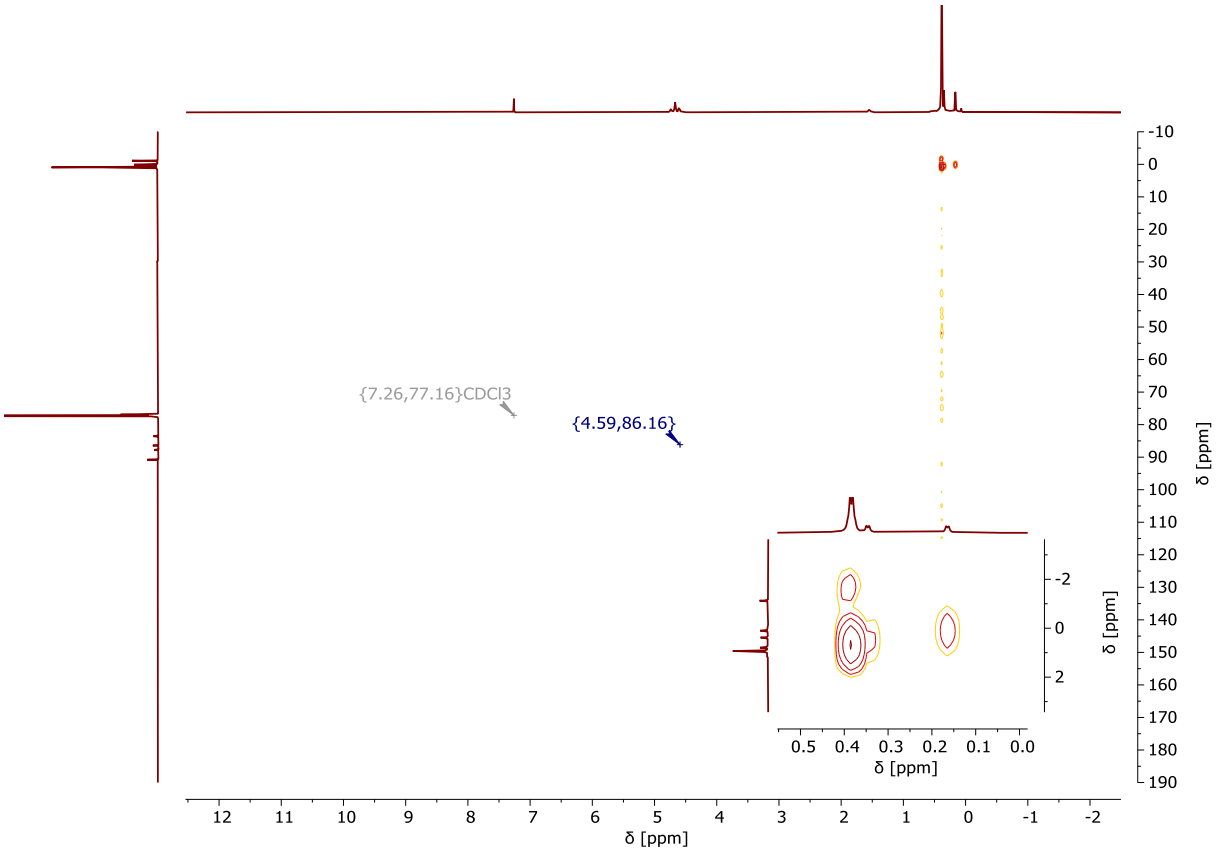


Figure 14. $^{1}H,^{13}C$ HMQC NMR spectrum.

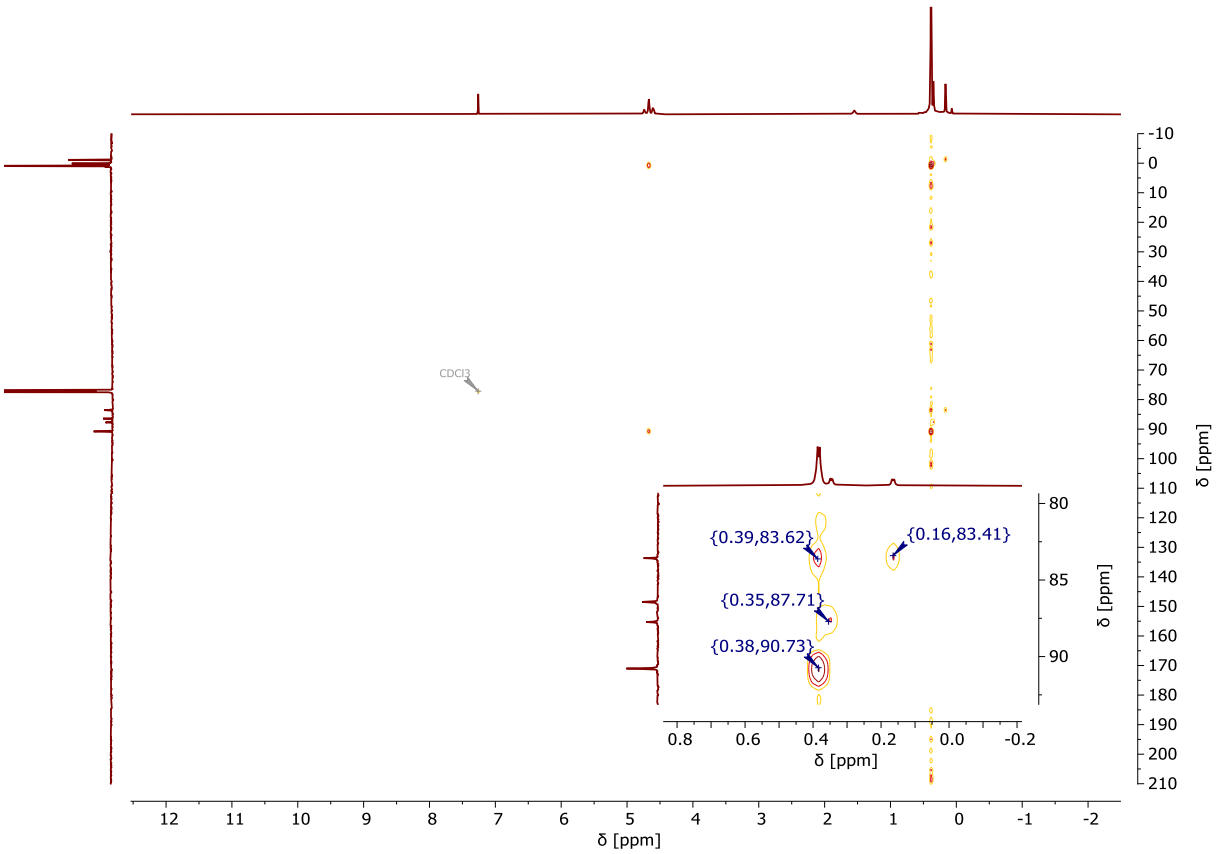


Figure 15. $^{1}H,^{13}C$ HMBC NMR spectrum.

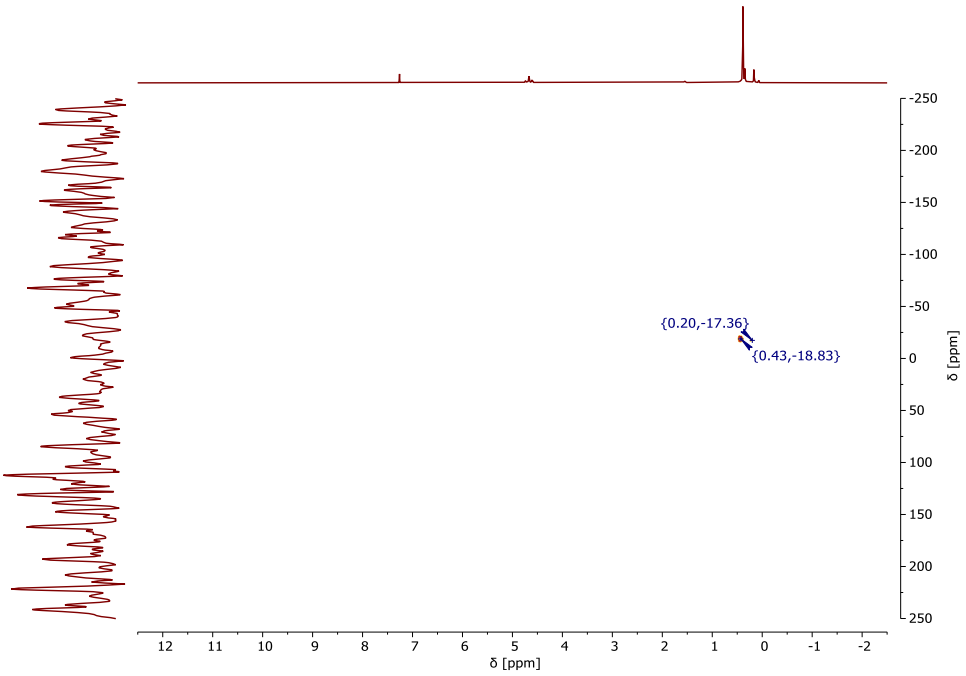


Figure 16. $^{1}H$, $^{29}Si$ HMBC NMR spectrum.

1,2,3,4,5-penta(dimethylsilyl)cyclopentadienyl-1,2,3-tri(dimethylsilyl)cyclopentadienyl-iron(II):

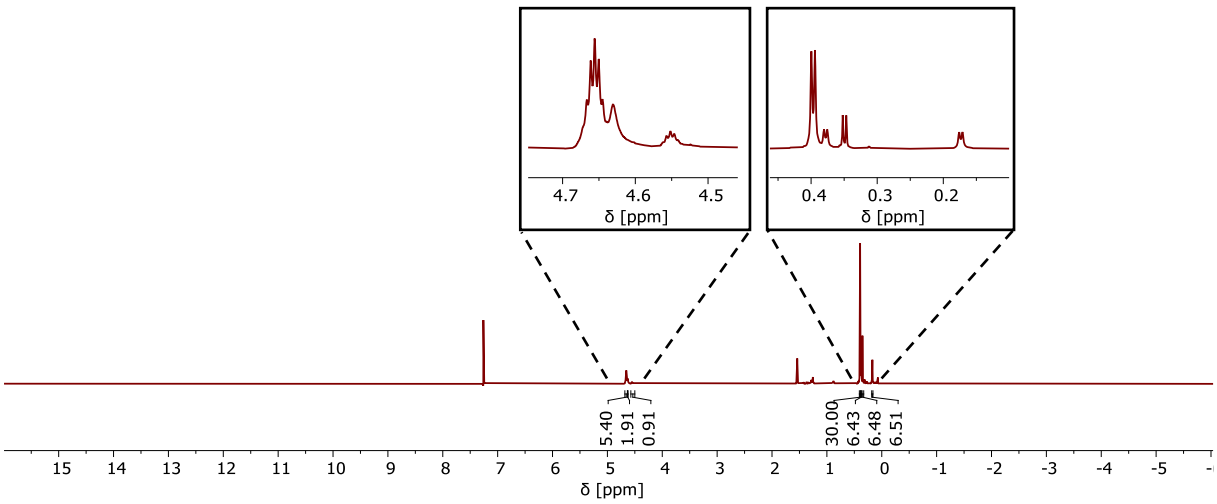


Figure S17. $^{1}H$ NMR spectrum (700 MHz, $CDCl_3$, RT).

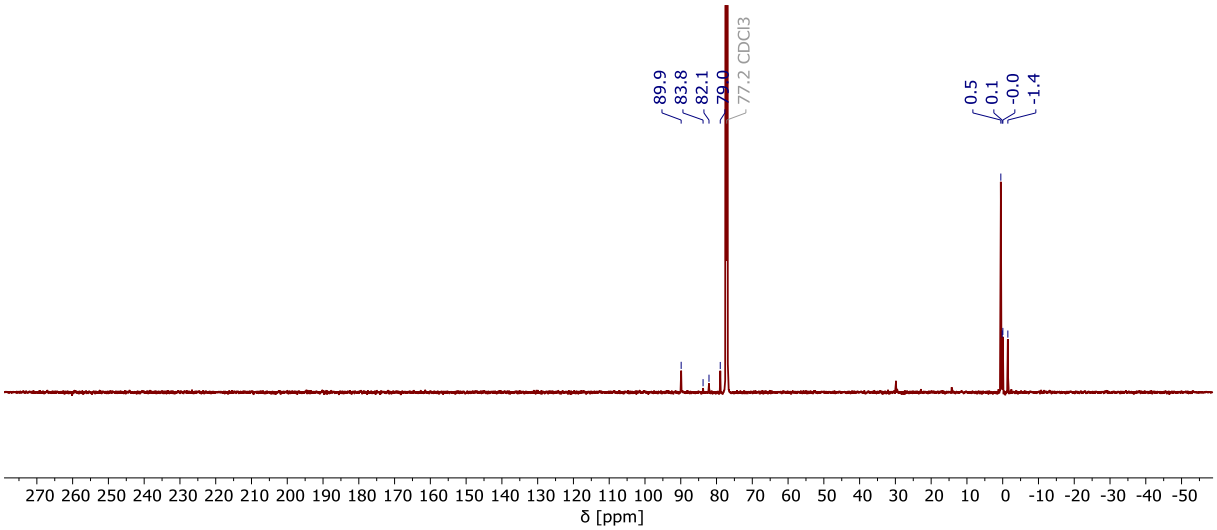


Figure S18. $^{13}C\{^{1}H\}$ NMR spectrum (176 MHz, $CDCl_3$, RT).

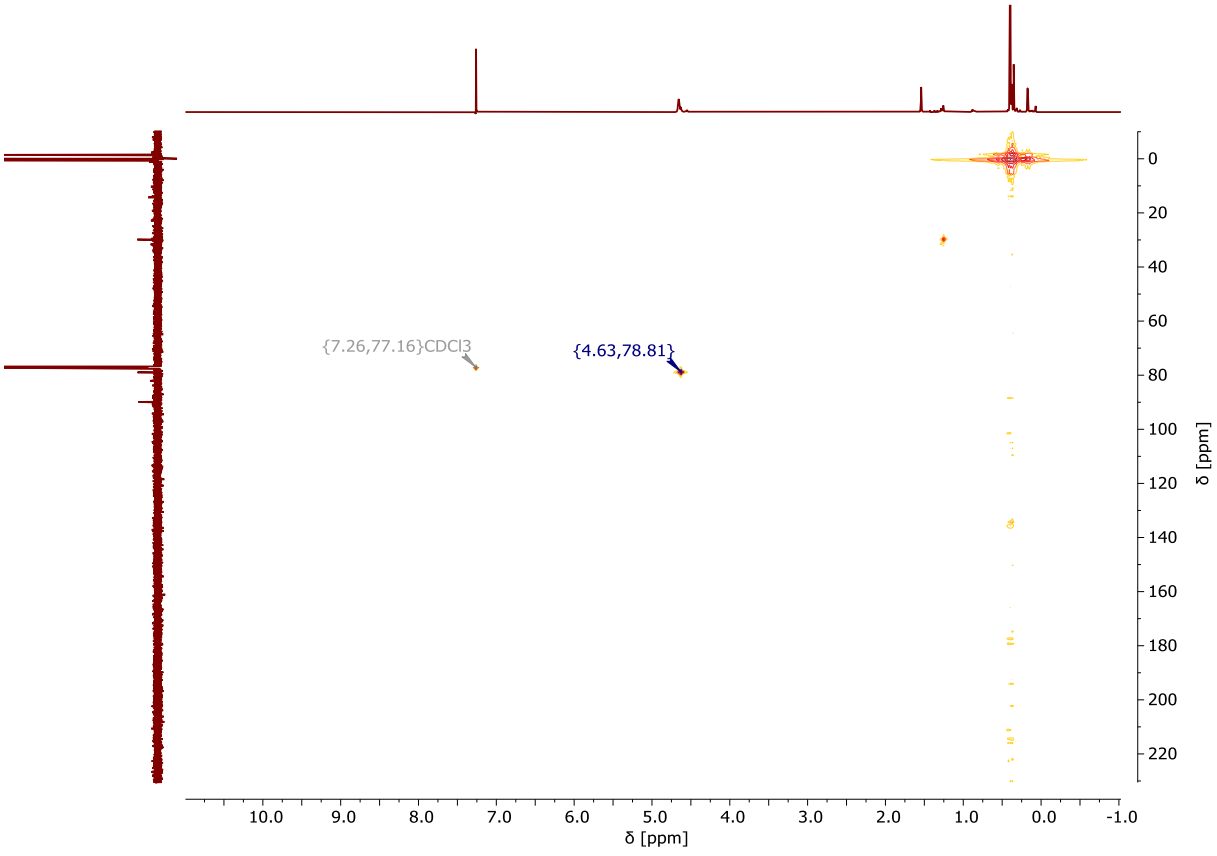


Figure S19. $^{1}H,^{13}C$ HMQC NMR spectrum.

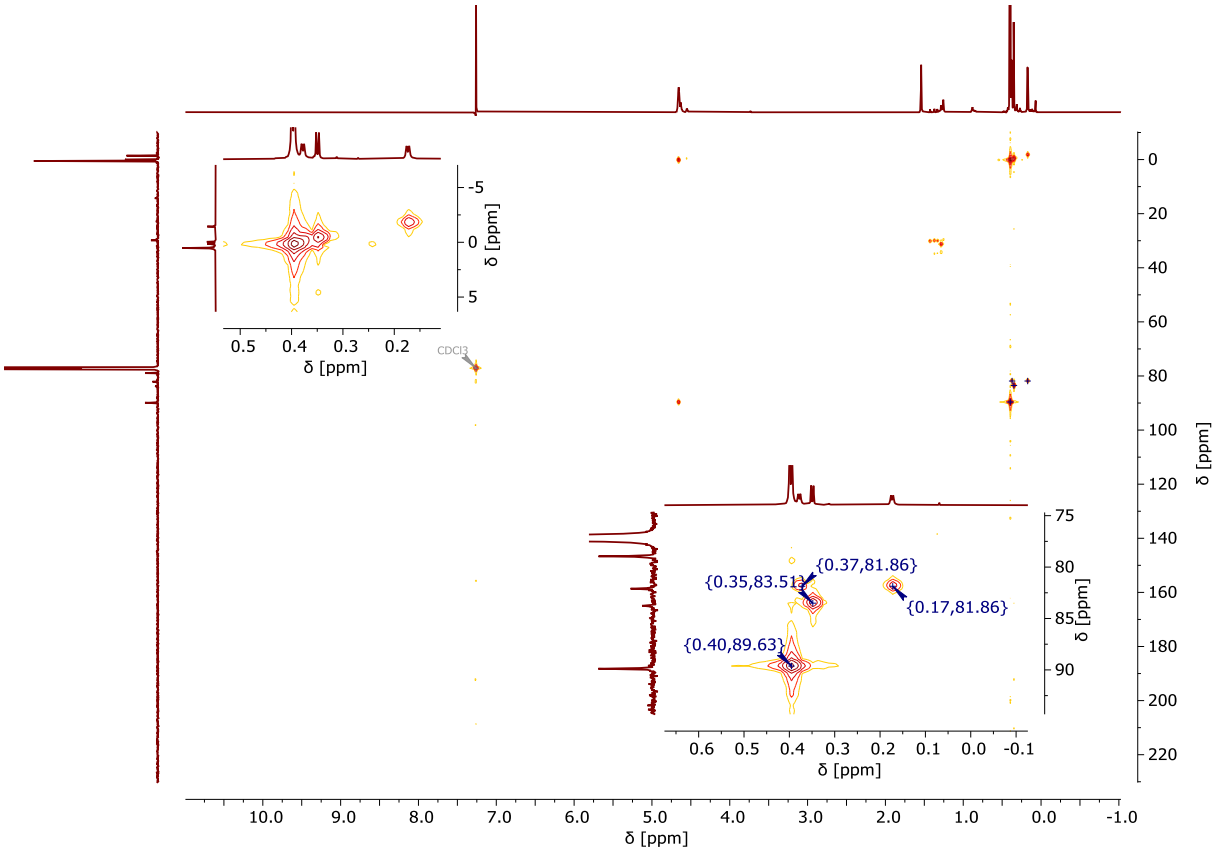


Figure S20. $^{1}H,^{13}C$ HMBC NMR spectrum.

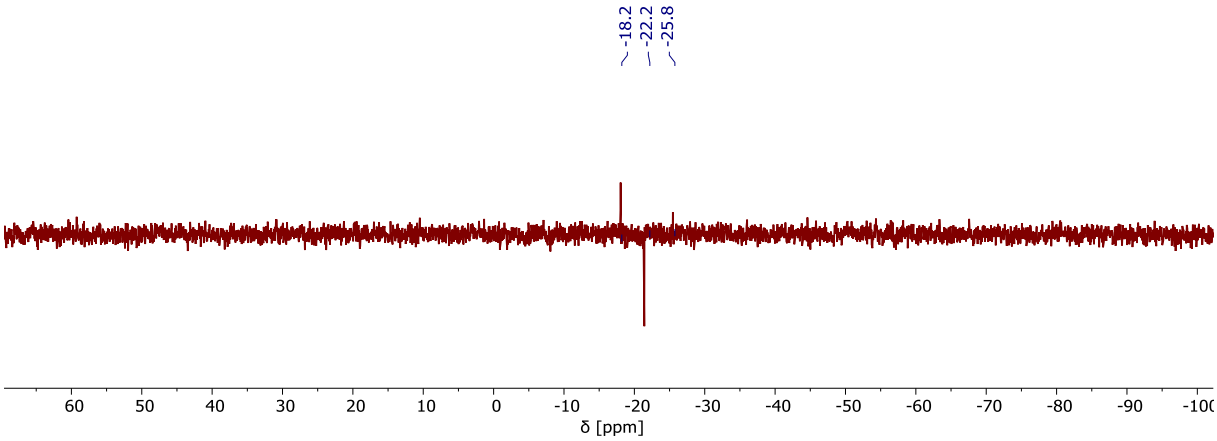


Figure S21. $^{29}Si$ DEPT spectrum ($CDCl_3$, RT, 80 MHz).

Bis(1,2,3,4-tetra(dimethylsilyl)cyclopentadienyl)iron(II):

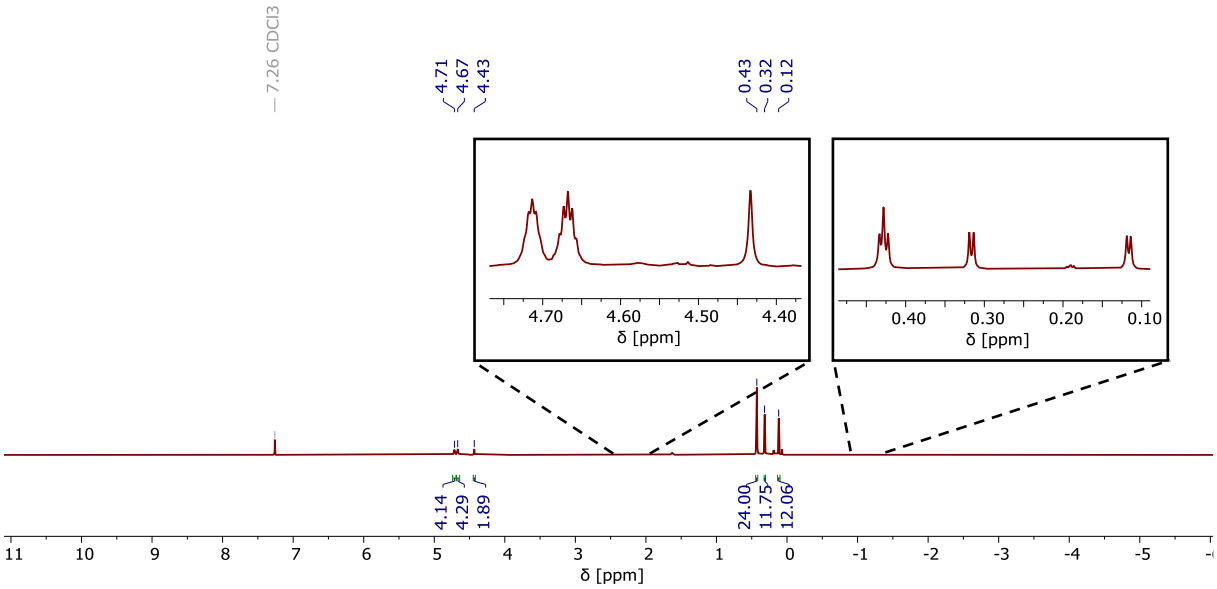


Figure S22. $^{1}H$ NMR spectrum (700 MHz, $CDCl_3$, RT).

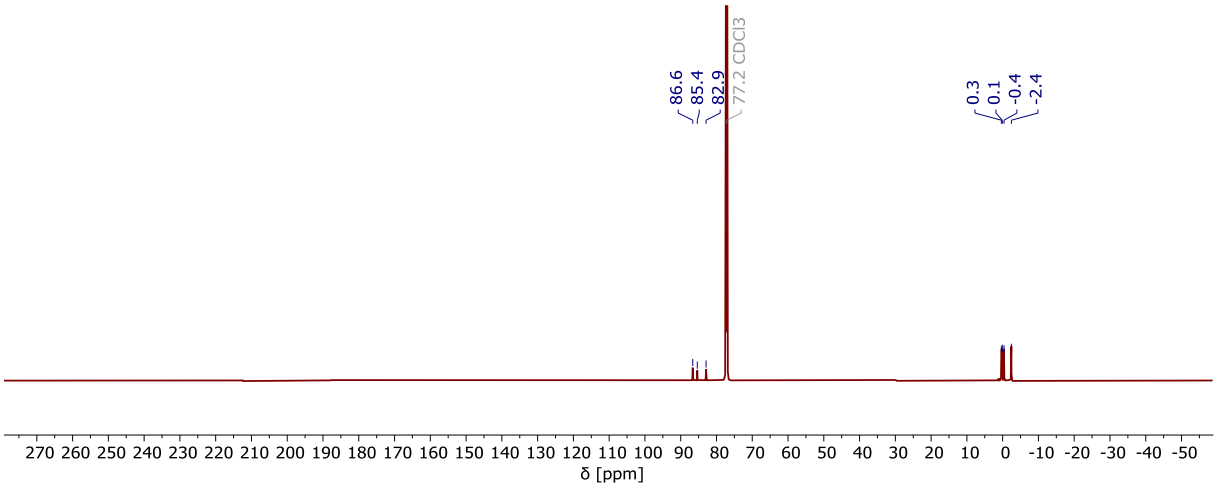


Figure S23. $^{13}C\{^{1}H\}$ NMR spectrum (176 MHz, $CDCl_3$, RT).

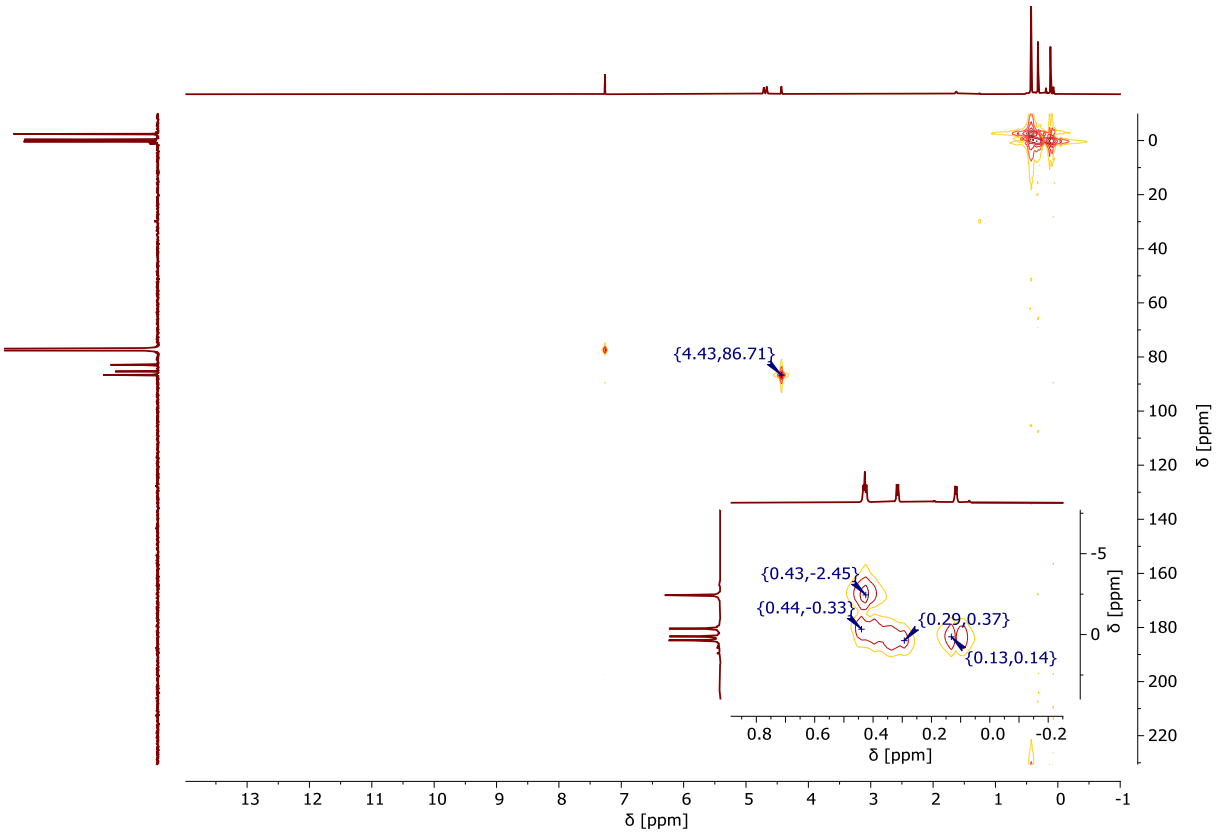


Figure S24. $^{1}H,^{13}C$ HMQC NMR spectrum.

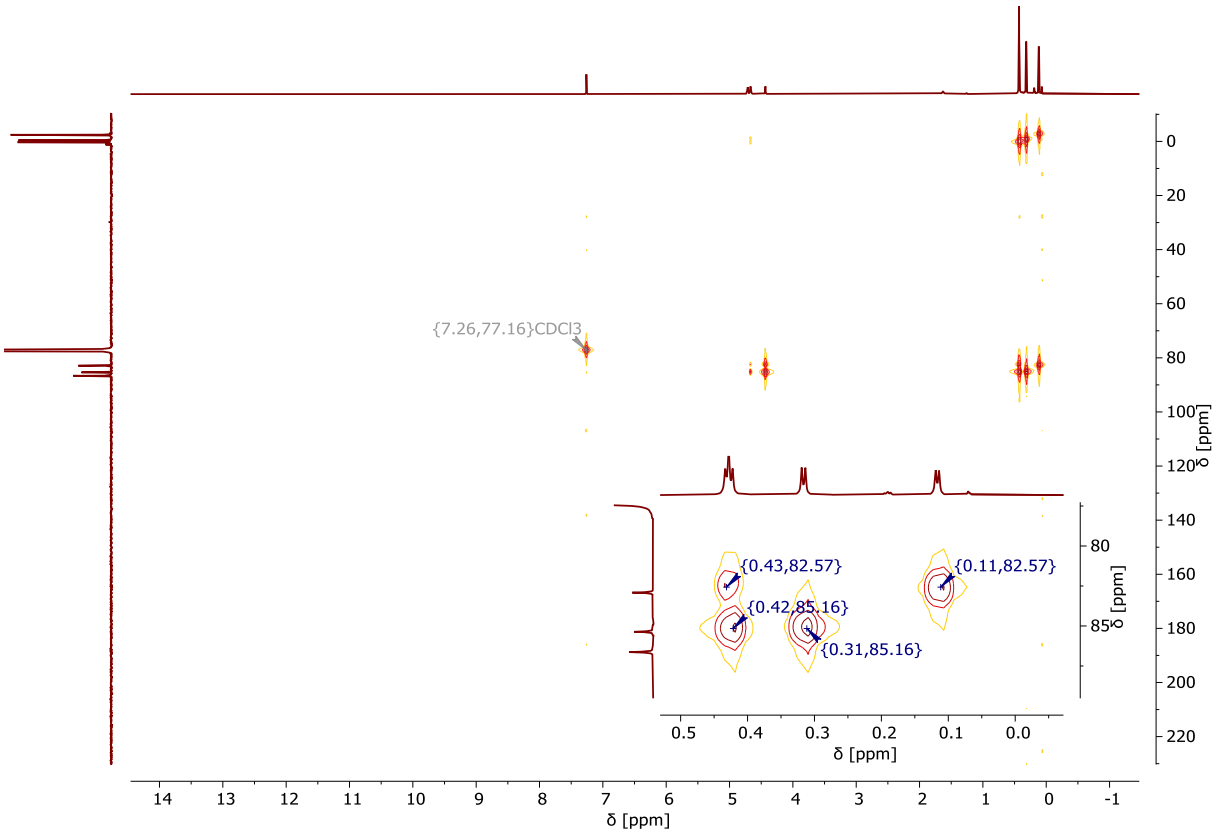


Figure S25. $^{1}H,^{13}C$ HMBC NMR spectrum.

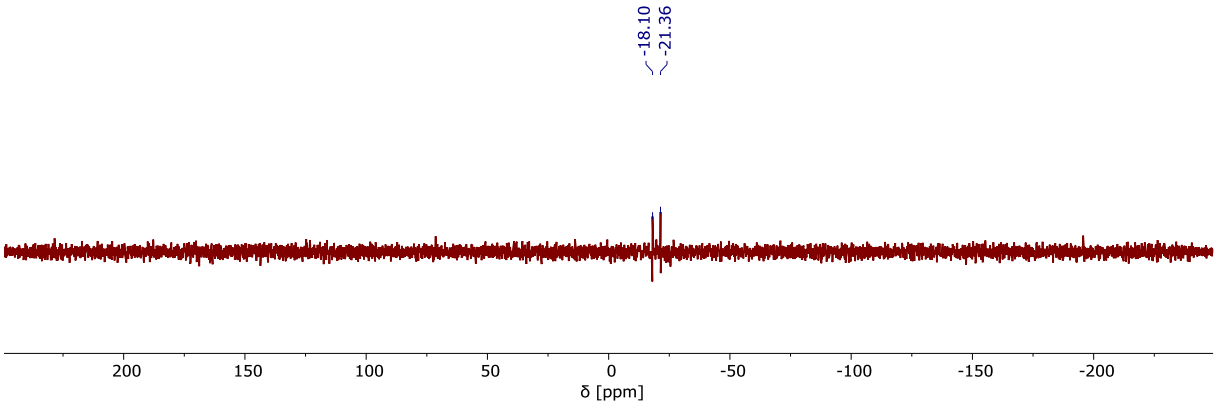


Figure S26. $^{29}$Si DEPT spectrum ($CDCl_3$, RT, 80 MHz).

## 1,2,3,4-tetra(dimethylsilyl)cyclopentadienyl-1,2,4-tri(dimethylsilyl)cyclopentadienyliron(II):

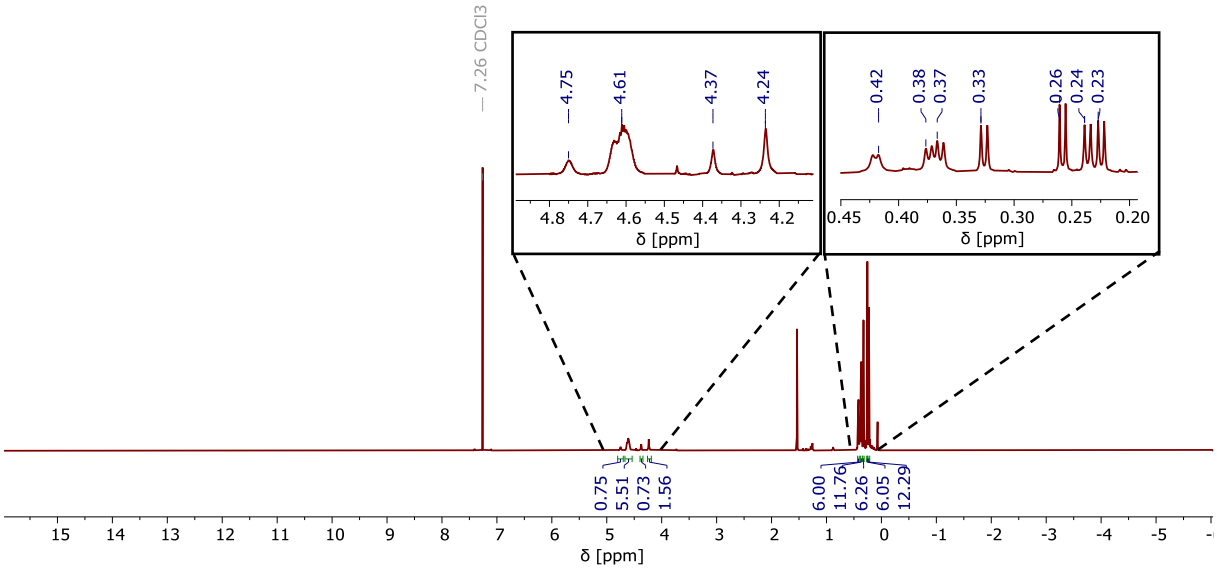


Figure S27. $^{1}$H NMR spectrum (700 MHz, $CDCl_3$, RT).

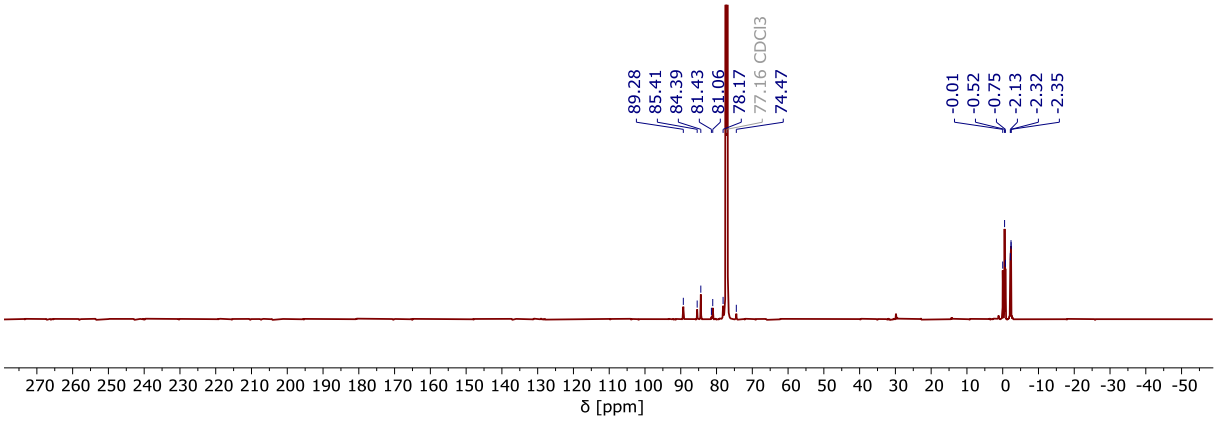


Figure S28. $^{13}$C{$^{1}$H} NMR spectrum (176 MHz, $CDCl_3$, RT).

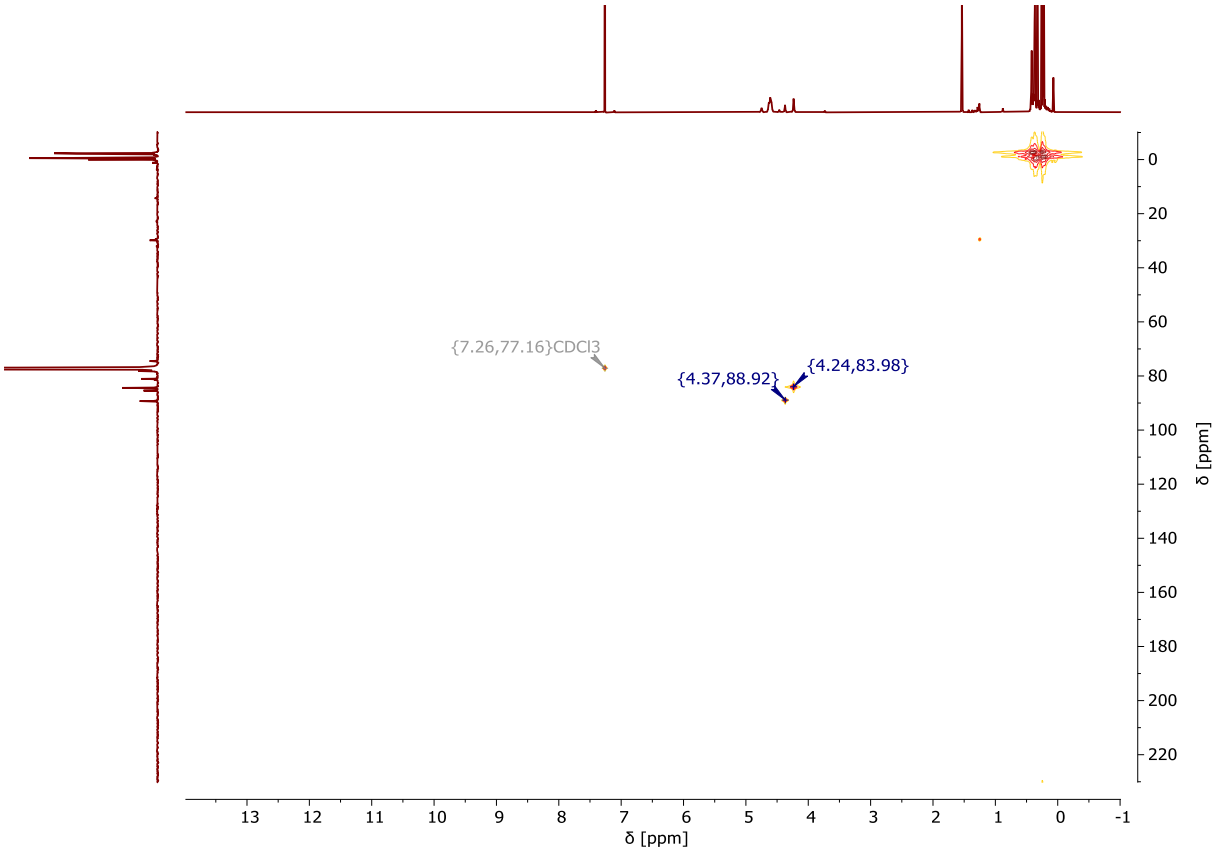


Figure S29. $^{1}H,^{13}C$ HMQC NMR spectrum.

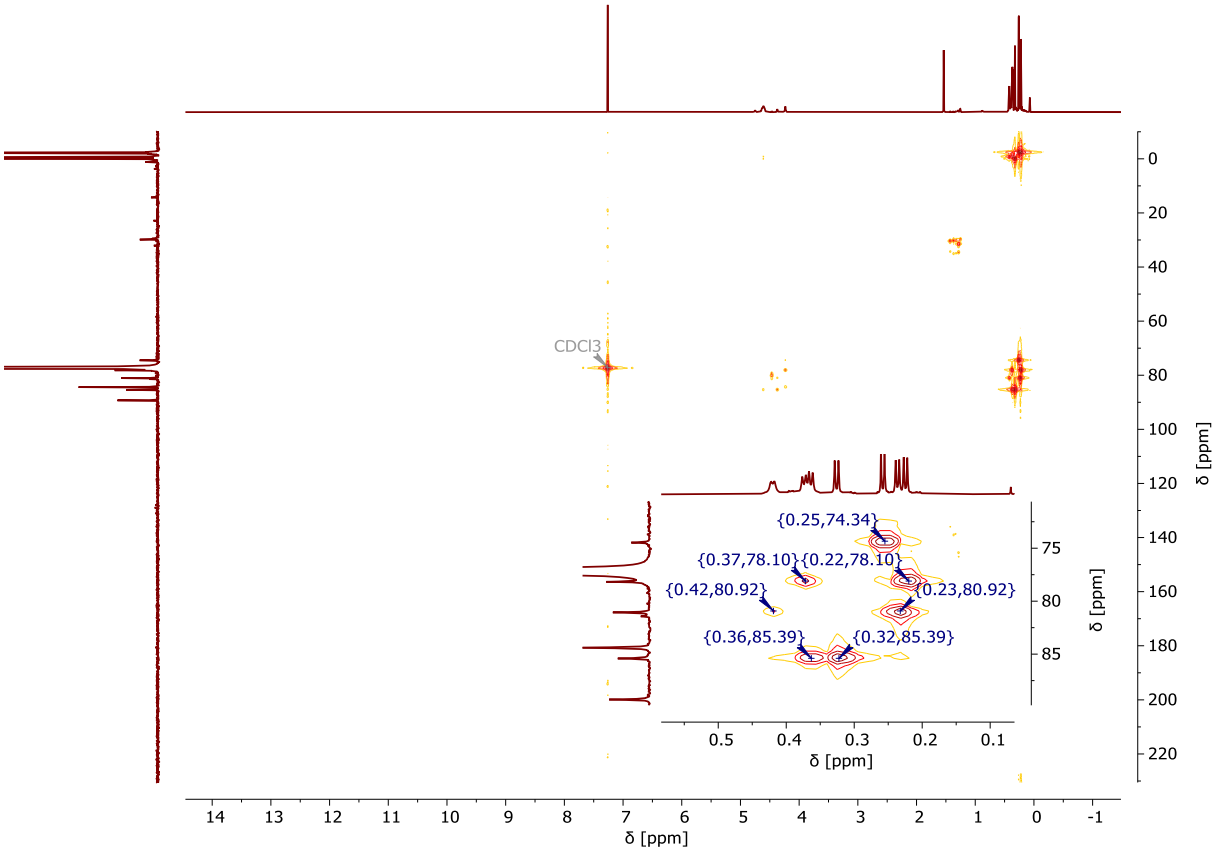


Figure S30. $^{1}H,^{13}C$ HMBC NMR spectrum.

1,2,3,4-tetra(dimethylsilyl)cyclopentadienyl-1,2,3-tri(dimethylsilyl)cyclopentadienyliron(II):

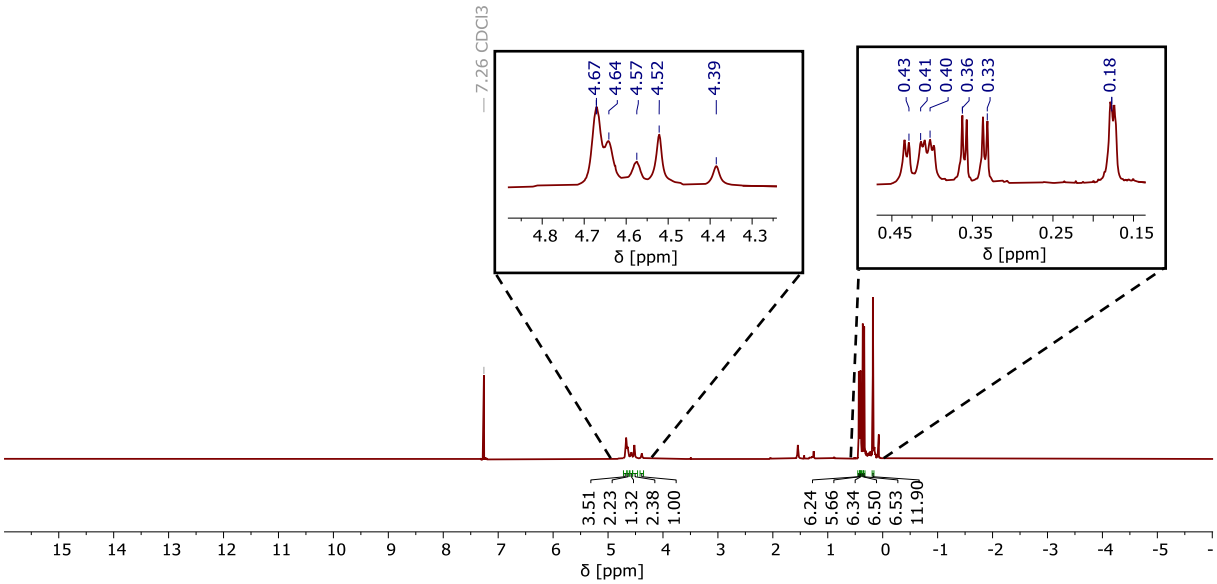


Figure S31. $^{1}$H NMR spectrum (700 MHz, $CDCl_3$, RT).

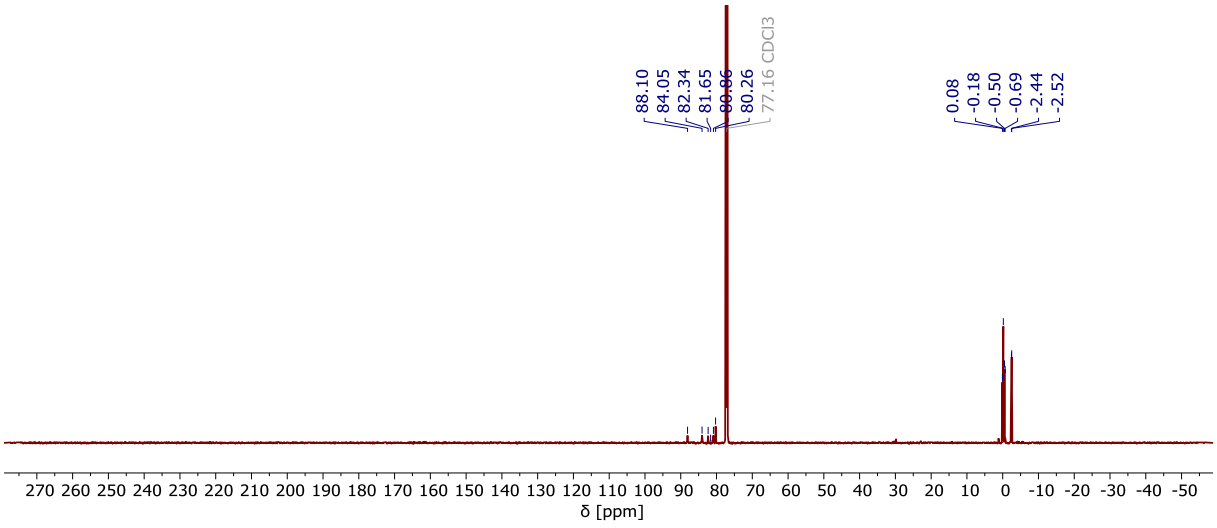


Figure S32. $^{13}C\{^{1}H\}$ NMR spectrum (700 MHz, $CDCl_3$, RT).

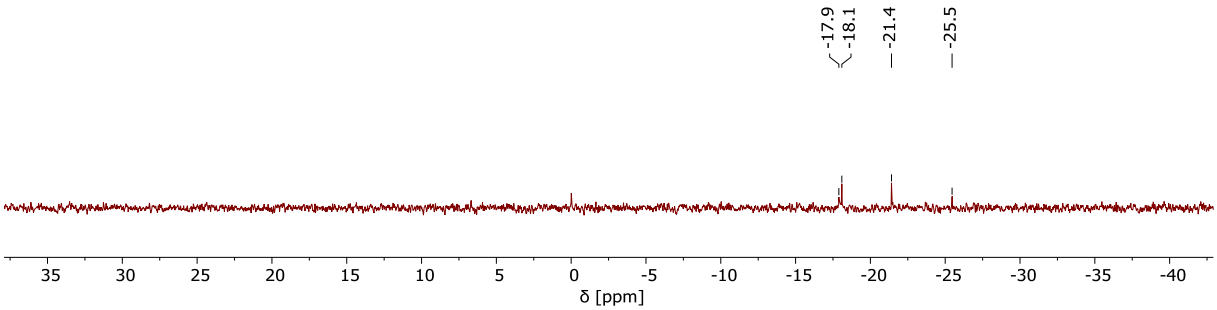


Figure S33. $^{29}Si\{^{1}H\}$ NMR spectrum (80 MHz, $CDCl_3$, RT).

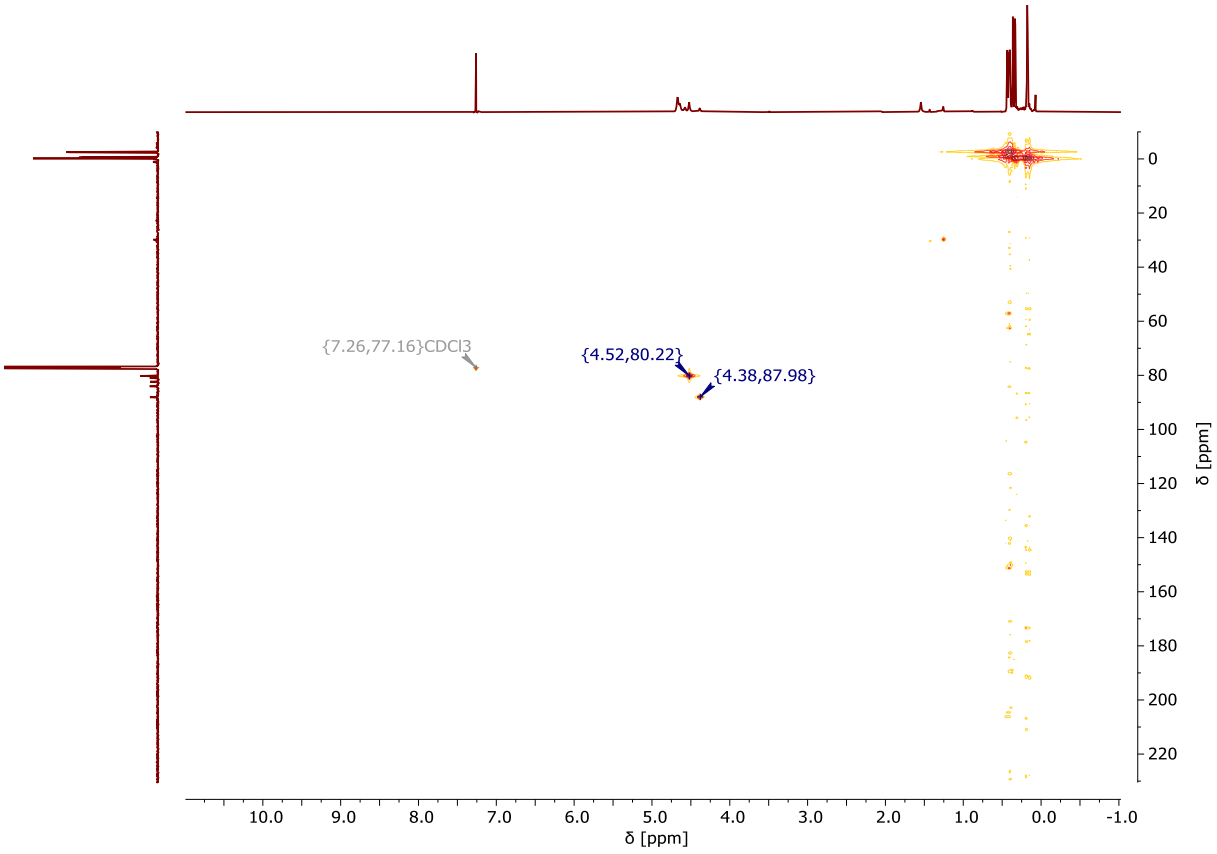


Figure S34. $^{13}C,^{1}H$ HMQC spectrum.

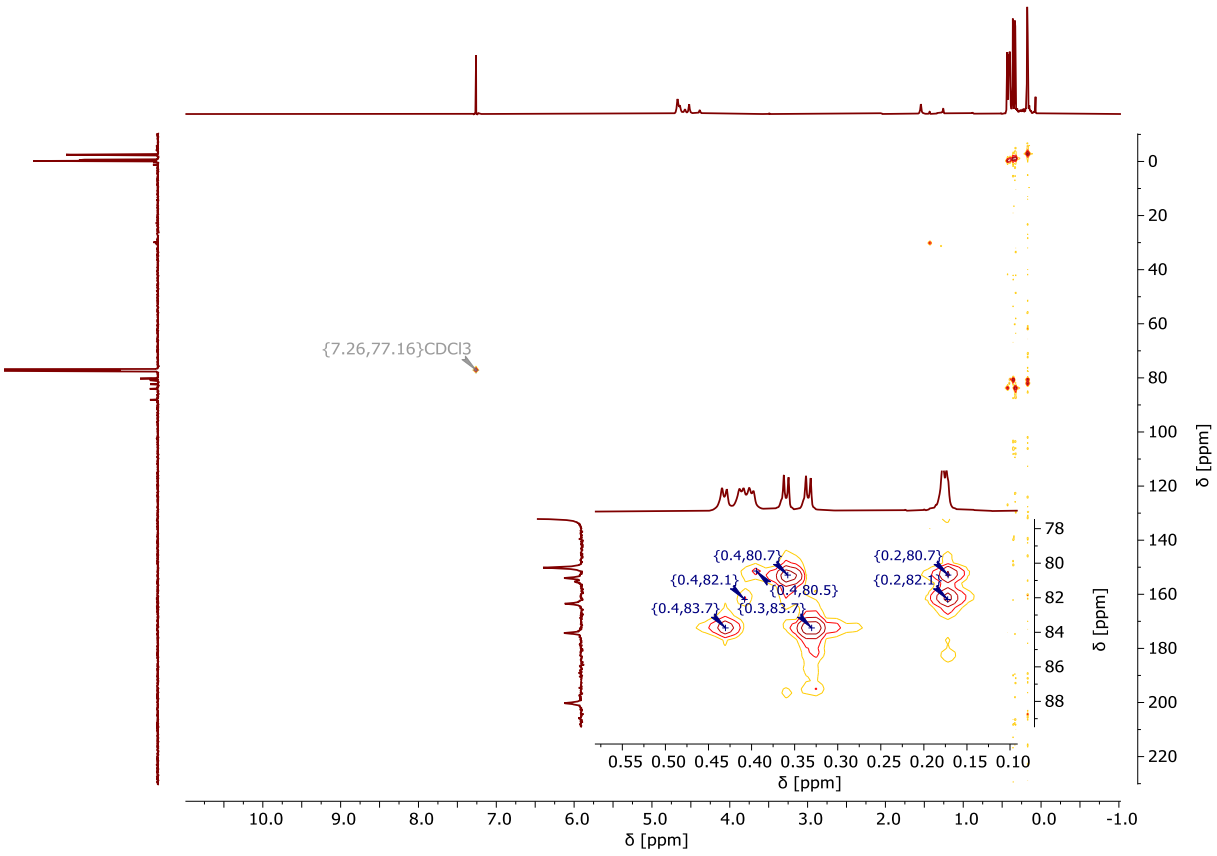


Figure S35. $^{13}C,^{1}H$ HMBC spectrum.

Bis(1-methyl-2,3,4,5-tetra-bromo-cyclopentadienyl)iron(II):

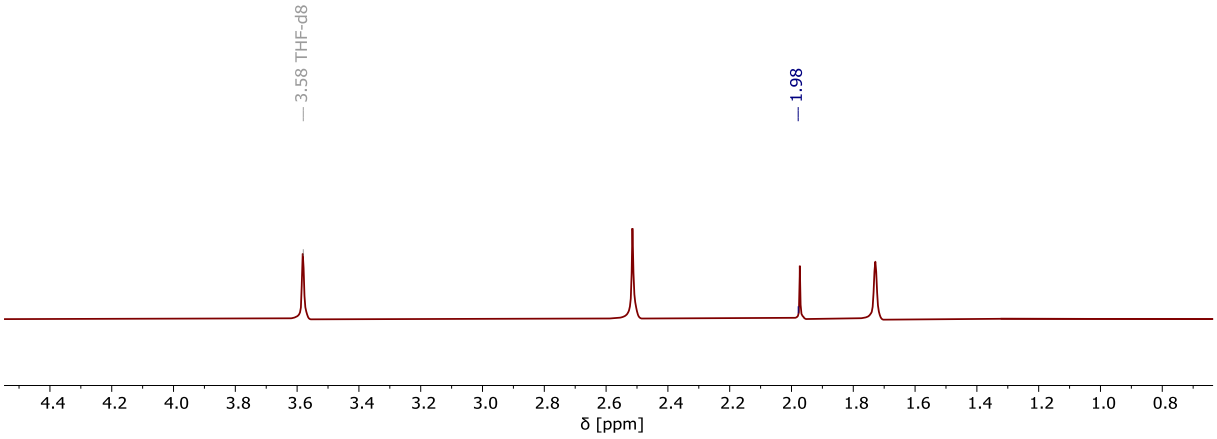


Figure S36. $^{1}$H NMR spectrum (700 MHz, $CDCl_3$, RT).

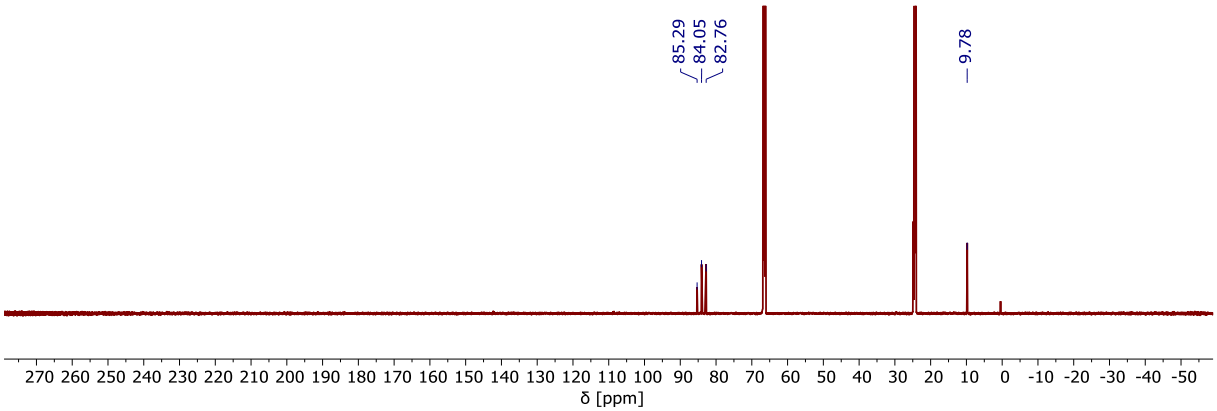


Figure S37. $^{13}C\{^{1}H\}$ NMR spectrum (700 MHz, $CDCl_3$, RT).

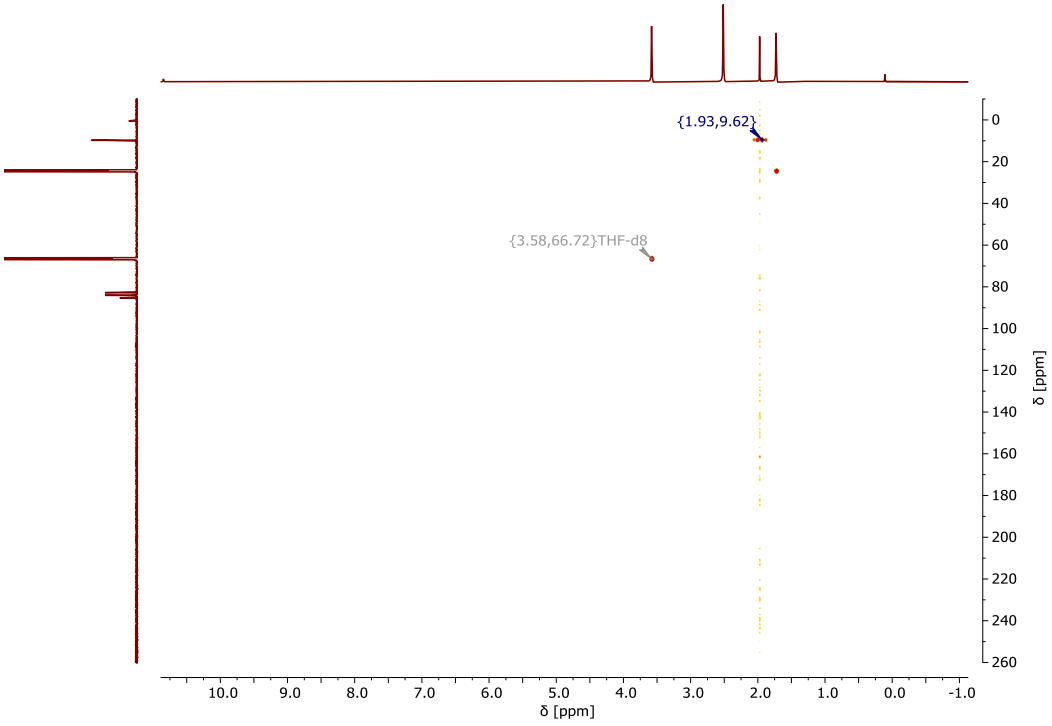


Figure S38. $^{13}C,^{1}H$ HMQC spectrum.

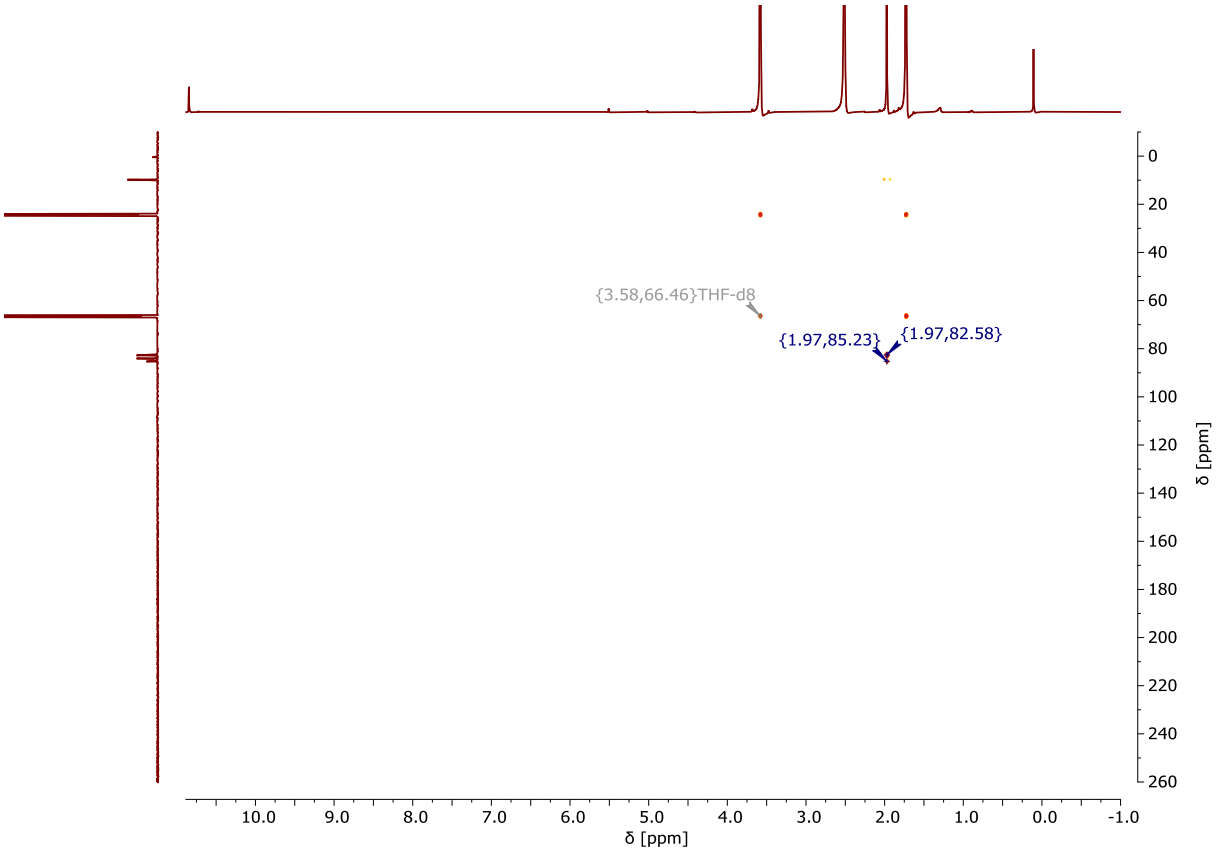


Figure S39. $^{13}C,^{1}H$ HMBC spectrum.

## Bis(1-methyl-2,3,4,5-tetra-dimethylsilyl-cyclopentadienyl)iron(II):

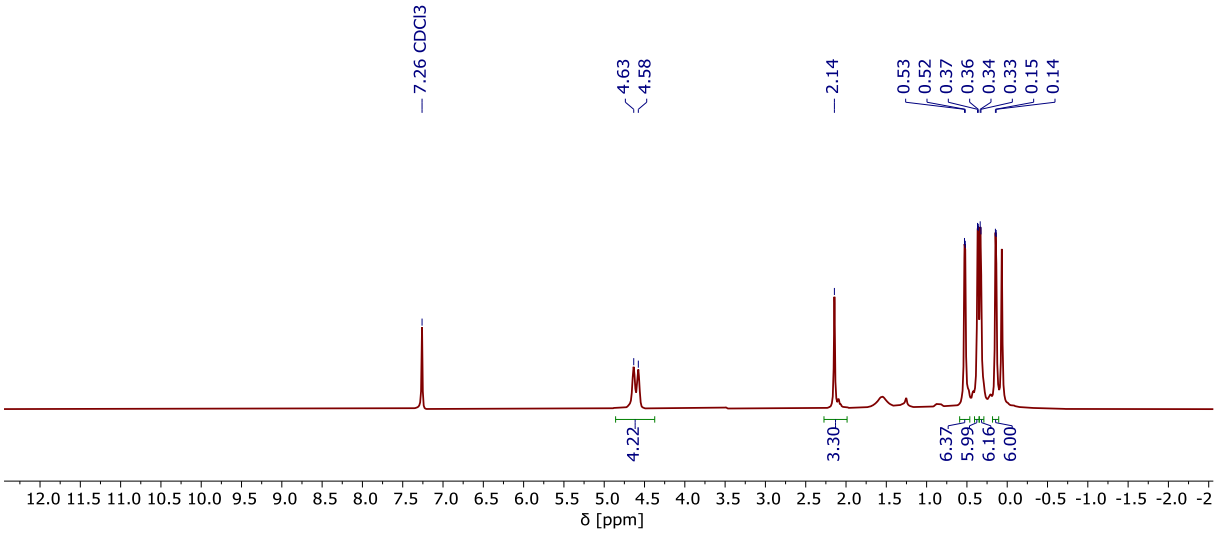


Figure S40. $^{1}H$ NMR spectrum (400 MHz, $CDCl_3$, RT).

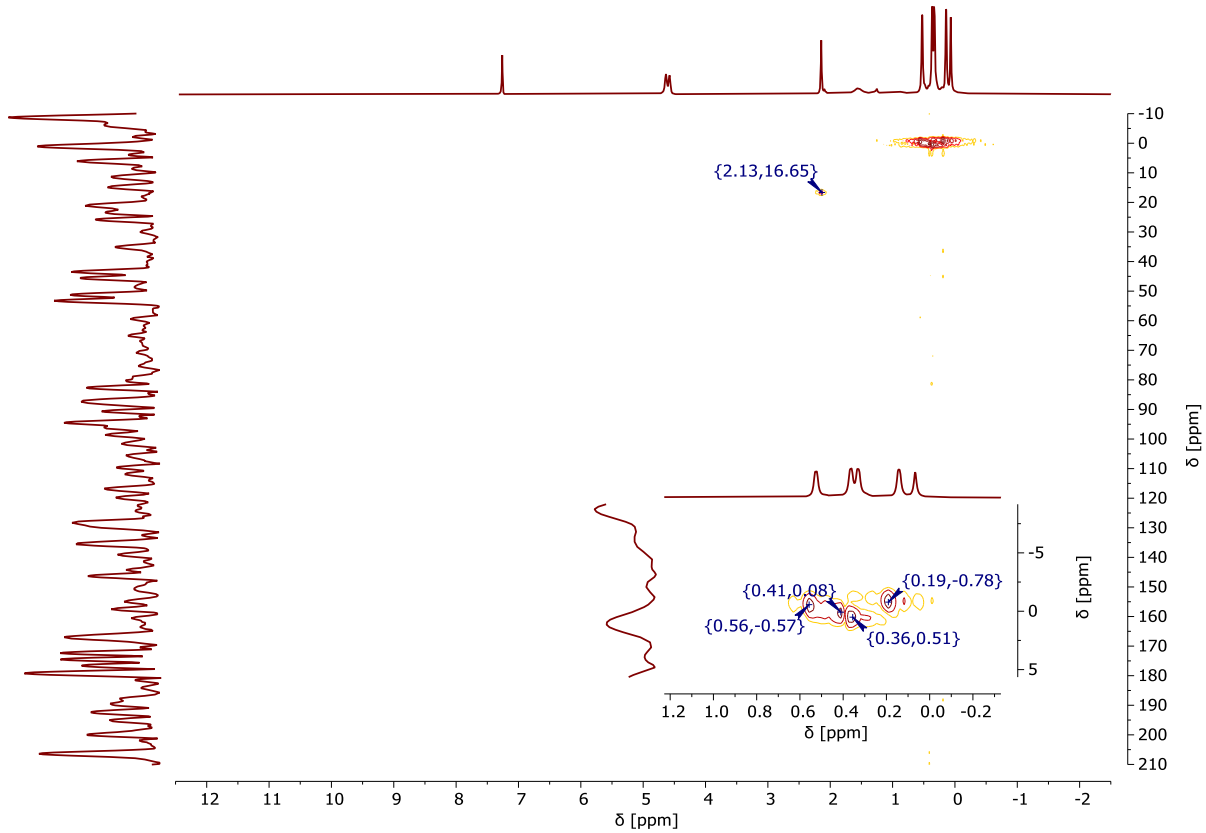


Figure S41. $^{13}C,^{1}H$ HMQC spectrum.

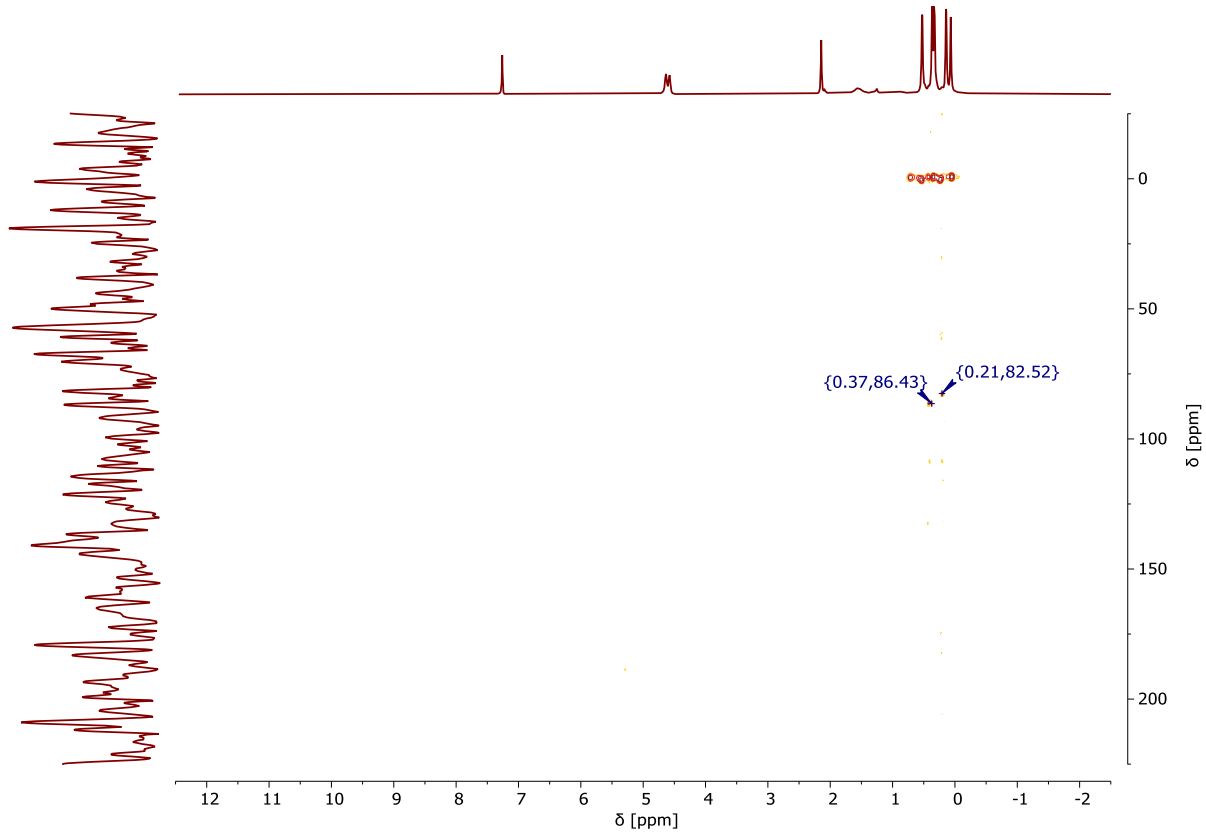


Figure S42. $^{13}C,^{1}H$ HMBC spectrum.

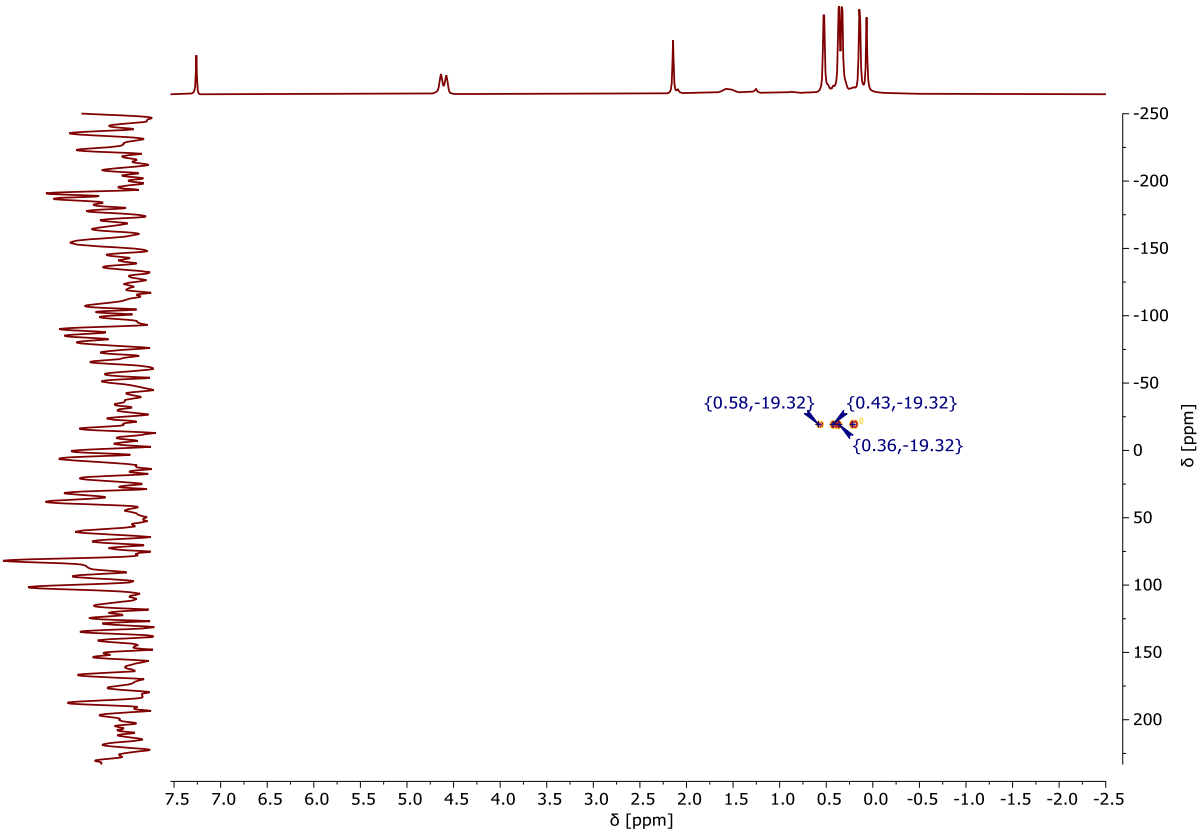


Figure S43. $^{1}H$, $^{29}Si$ HMBC NMR spectrum.

## 5.2 Infrared

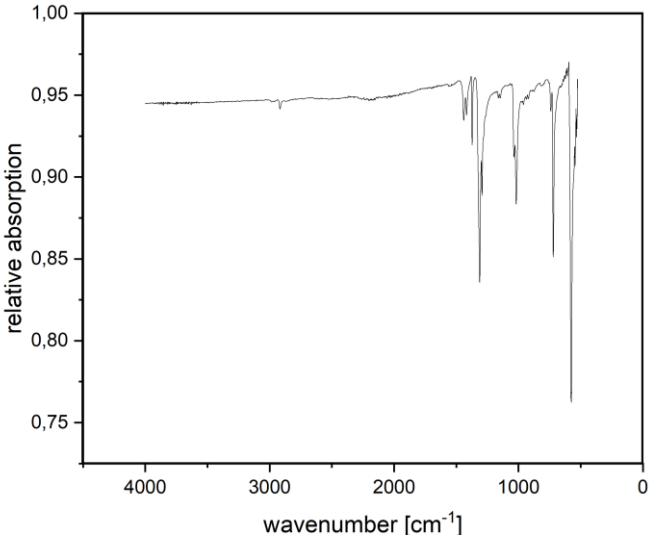


**Figure S44.** Infrared spectrum (ATR) of compound $[FeC_{10}Me_2Br_8]$ (**7**).

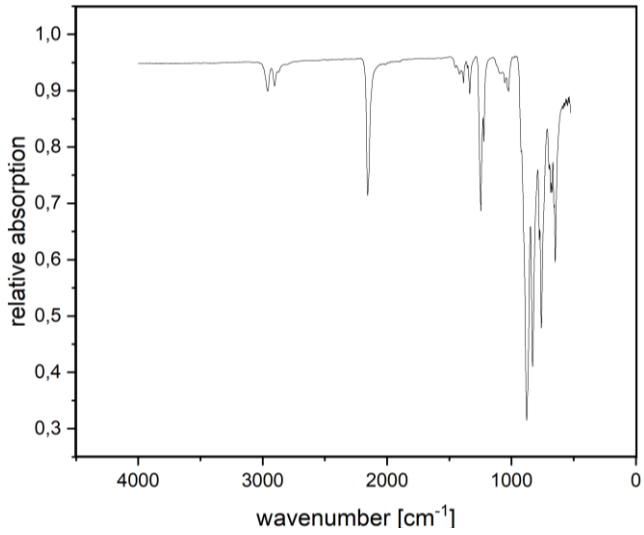


Figure S45. Infrared spectrum (ATR) of compound [$FeC_{10}Me_2DMS_8$] (**8**).

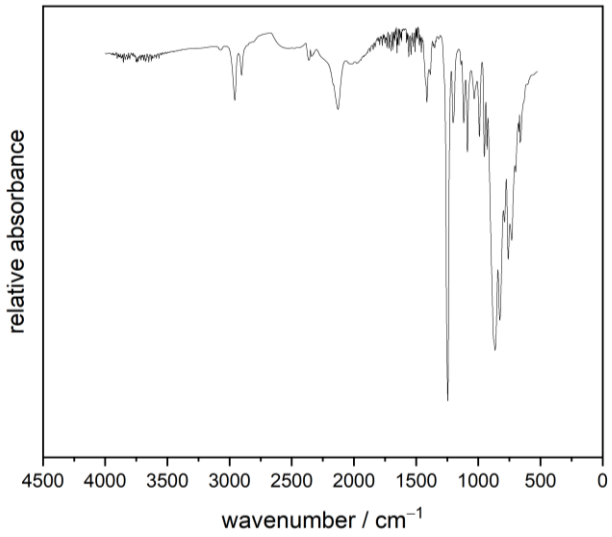


Figure S46. Infrared spectrum (ATR) of compound [$FeC_{10}DMS_7H_3$] (**3a**).

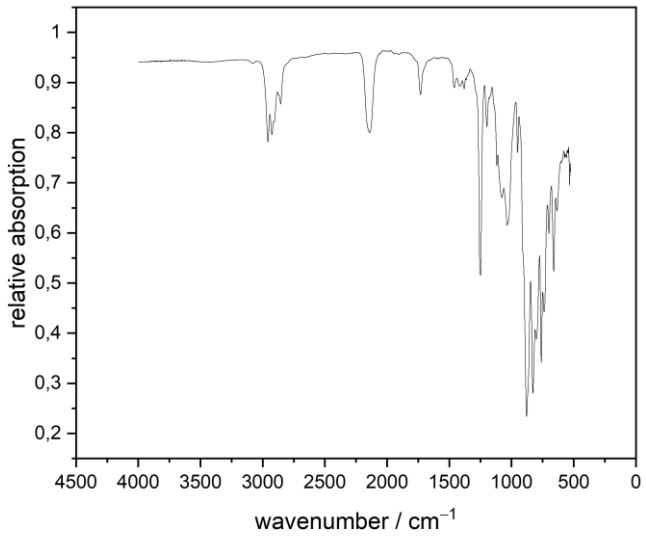


Figure S47. Infrared spectrum (ATR) of compound [$FeC_{10}DMS_7H_3$] (**3b**).

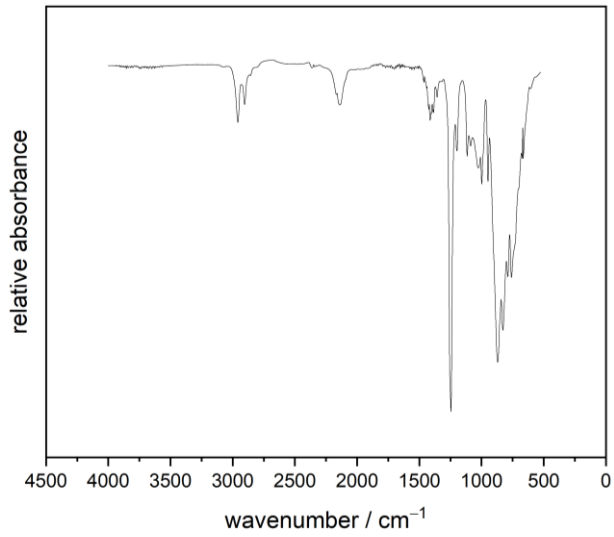


Figure S48. Infrared spectrum (ATR) of compound [$FeC_{10}DMS_8H_2$] (**4a**).

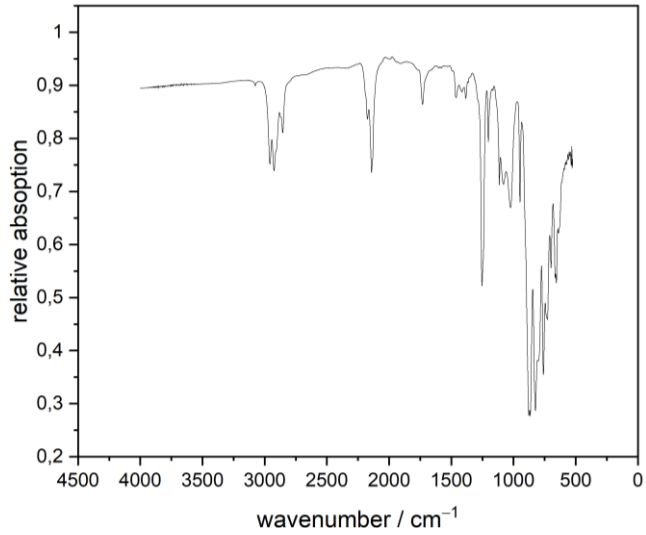


Figure S49. Infrared spectrum (ATR) of compound [$FeC_{10}DMS_8H_2$] (**4b**).

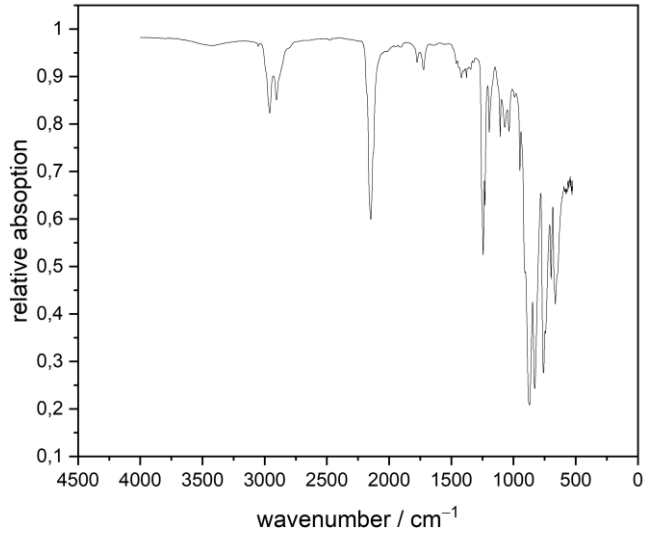


Figure S50. Infrared spectrum (ATR) of compound [$FeC_{10}DMS_9H$] (**5**).

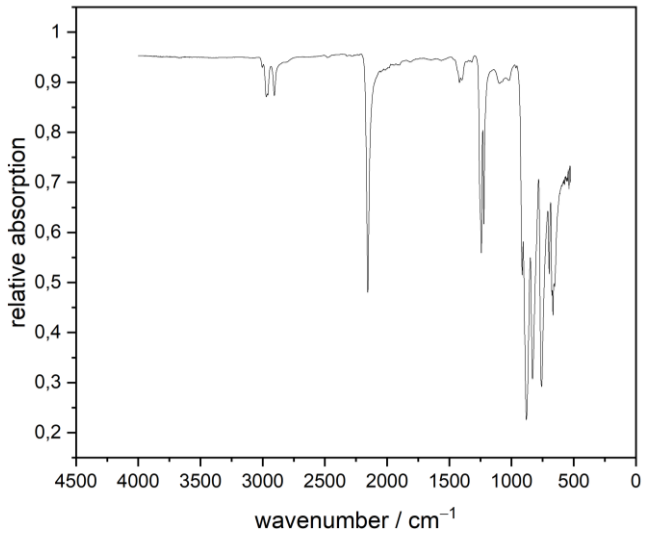


Figure S51. Infrared spectrum (ATR) of compound [$FeC_{10}DMS_{10}$] (**6**).

## 5.3 Cyclic voltammetry

Cyclic voltammetry was performed on a Interface 1010 B Potentiostat/Galvanostat/ZRA from Gamry Instruments. The investigations were carried out starting from 0 V going to the oxidation first and then to the reduction. The measurements were performed in anhydrous and oxygen free solvents under argon atmosphere using tetrabutylammonium hexafluorophosphate as the supporting electrolyte and platinum wires as working-, counter-, and quasi-reference electrodes. The voltammograms were internally referenced against $FeCp_2^{0/+}$. The software OriginPro 2017G was used to plot the data.[8] THF was distilled over Na and stored in Young flasks under argon atmosphere over molar sieve (3 Å) which was dried beforehand at 250 °C under high vacuum. The conducting salt was dried at 250 °C under high vacuum. The solvents were condensed on the conducting salt in the cyclic voltammetry cells via a vacuum line.

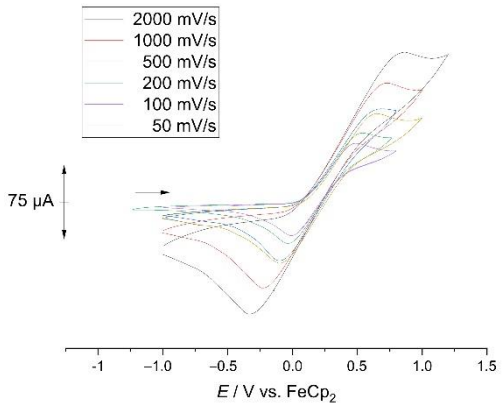


Figure S52. Cyclic voltammogram of compound [$FeC_{10}DMS_7H_3$] (**3b**) measured in tetrahydrofuran at 100 mV/s scan rate and [TBA][$PF_6$] as supporting electrolyte.

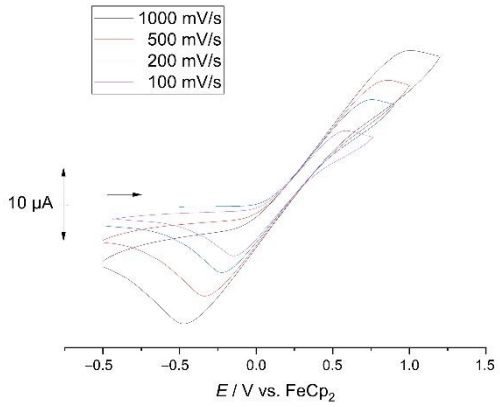


Figure S53. Cyclic voltammogram of compound [$FeC_{10}DMS_8H_2$] (**4b**) measured in tetrahydrofuran at 100 mV/s scan rate and [TBA][$PF_6$] as supporting electrolyte.

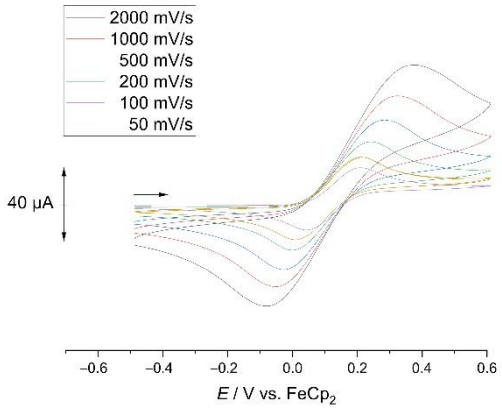


Figure S54. Cyclic voltammogram of compound [$FeC_{10}DMS_9H$] (**5**) measured in tetrahydrofuran at 100 mV/s scan rate and [TBA][$PF_6$] as supporting electrolyte.

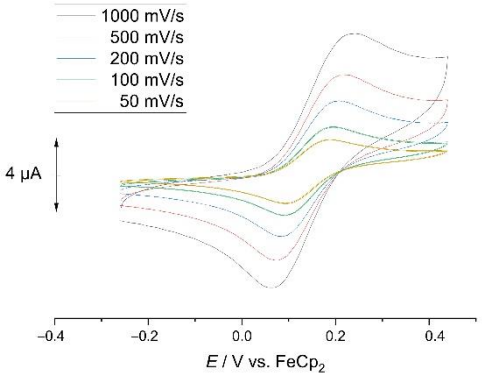


Figure S55. Cyclic voltammogram of compound [$FeC_{10}DMS_{10}$] (**6**) measured in tetrahydrofuran at 100 mV/s scan rate and [TBA][$PF_6$] as supporting electrolyte.

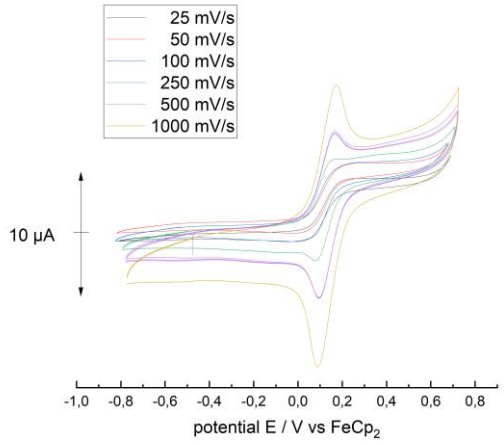


Figure S56. Cyclic voltammogram of compound [$FeC_{10}DMS_8Me_2$] (**8**) measured in tetrahydrofuran at 100 mV/s scan rate and [TBA][$PF_6$] as supporting electrolyte.

Table S4. Electrochemical data.

| **Compound** | $E_{pa}$ / V | $E_{pc}$ / V | $E_{1/2}$ / V | $\Delta E$ / mV |
|---|---|---|---|---|
| 6 (10x DMS) | 0.216 | 0.128 | 0.172 | 88 |
| 5 (9 x DMS) | 0.272 | 0.064 | 0.168 | 208 |
| 4b (8x DMS) | 0.407 | −0.067 | 0.170 | 474 |
| 3b (7x DMS) | 0.448 | −0.126 | 0.161 | 574 |
| 8 [$FeC_{10}DMS_8Me_2$] | 0.308 | −0.023 | 0.131 | 331 |

## 5.4 Mass Spectra

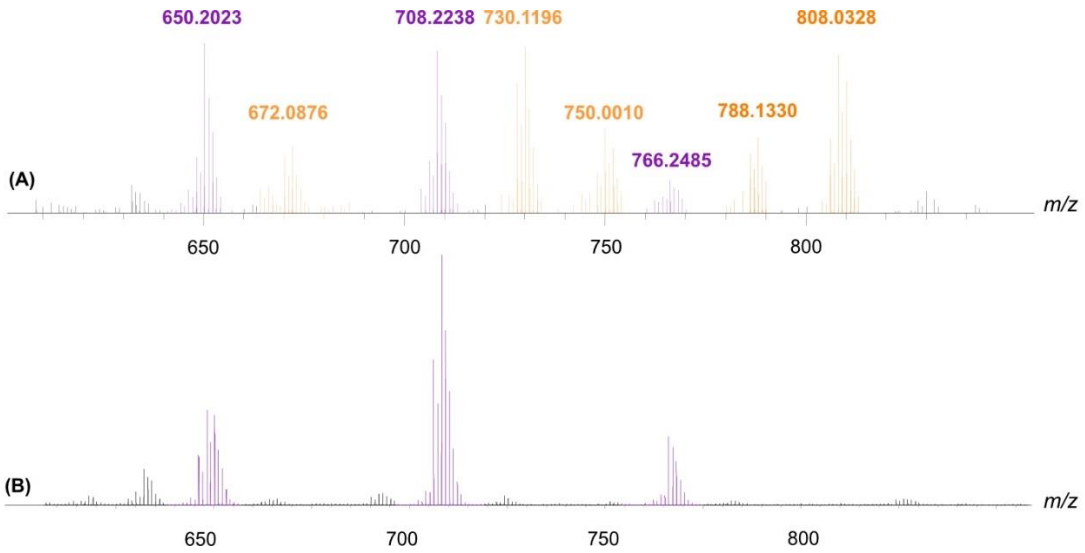


Figure S57. EI MS (+) after reaction of decabromoferrocene with $^t$BuLi and DMSCl in *n*-pentane (A) followed by reaction with $^t$BuLi and DMSCl in THF (B). Highlighted signals were assigned to purely silylated metallocenes (purple) or to partially brominated species (orange).

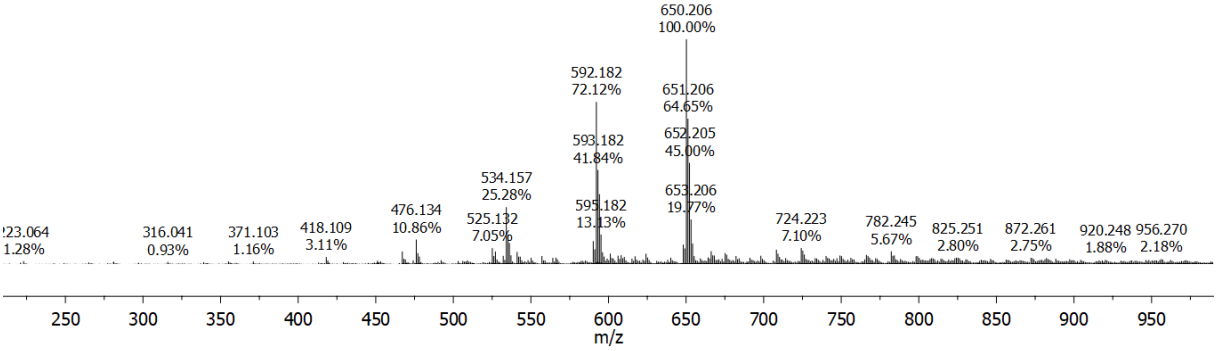


Figure S58. ESI MS (+) of entry 1 (Grignard).

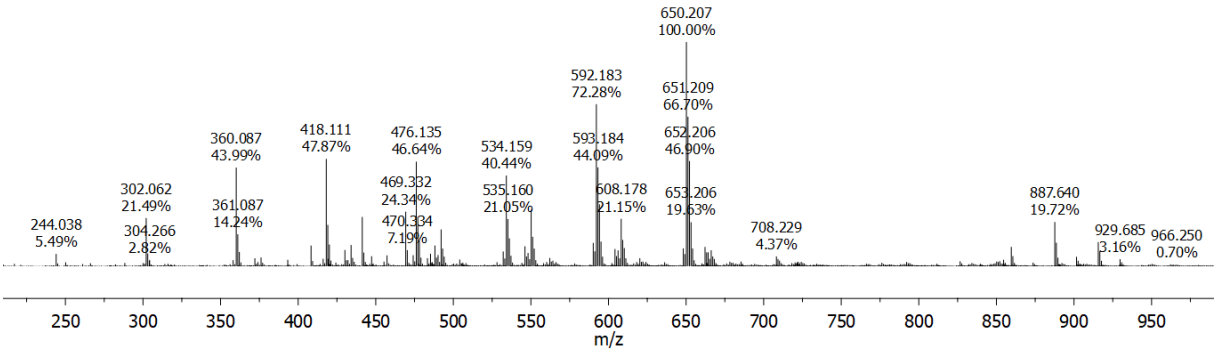


Figure S59. ESI MS (+) of entry 2 (Grignard).

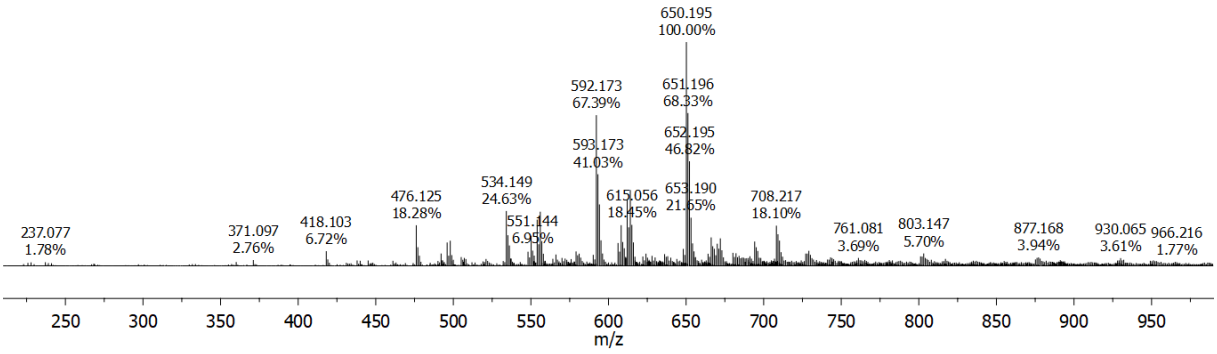


Figure S60. ESI MS (+) of entry 3 (Grignard).

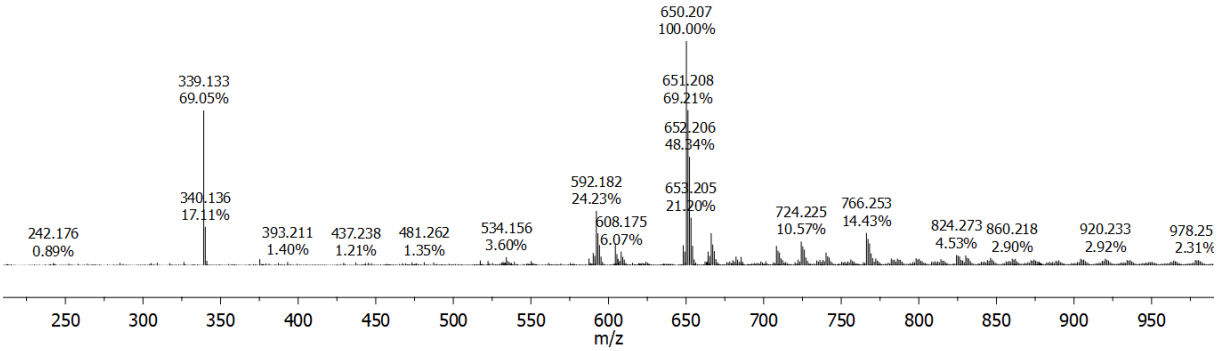


Figure S61. ESI MS (+) of entry 3 (Grignard).

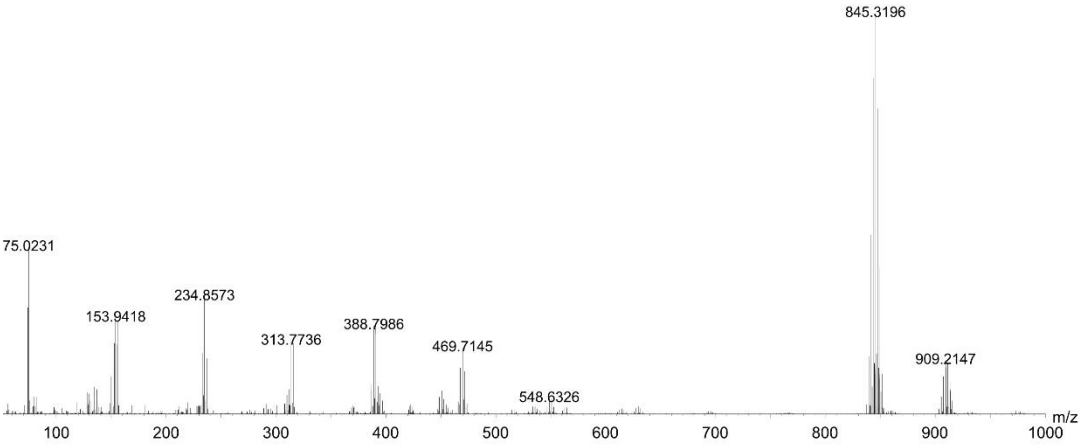


Figure S62. EI MS (+) spectrum of [$FeC_{10}Me_2Br_8$] (**7**).

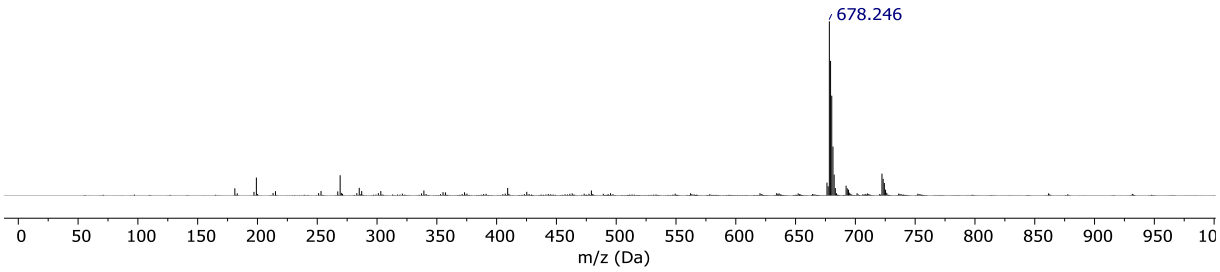


Figure S63. ESI MS (+) spectrum of [$FeC_{10}Me_2DMS_8$] (**8**).

## 5.5 UV/VIS

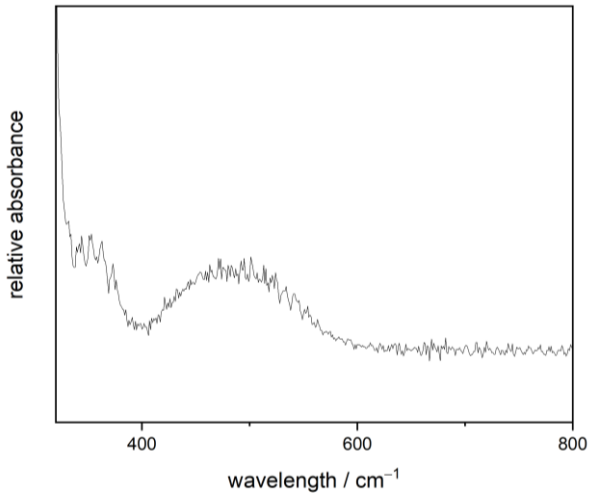


Figure S64. UV/VIS spectrum of [$FeC_{10}DMS_7H_3$] (**3a**) in *n*-pentane. $\lambda_{max}$ = 501 nm.

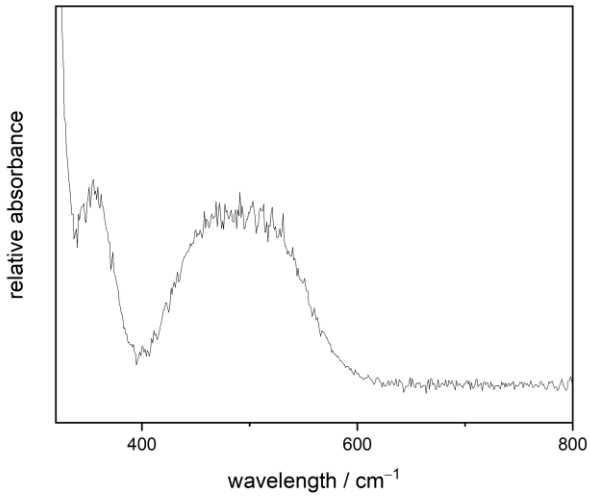


Figure S65. UV/VIS spectrum of [$FeC_{10}DMS_7H_3$] (**3b**) in *n*-pentane. $\lambda_{max}$ = 491 nm.

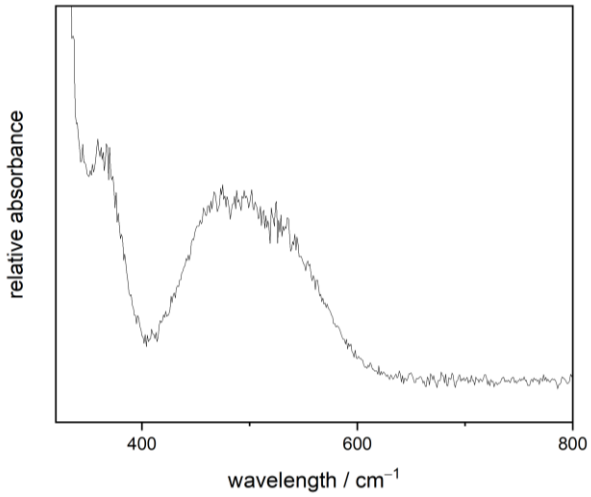


Figure S66. UV/VIS spectrum of [$FeC_{10}DMS_8H_2$] (**4a**) in *n*-pentane. $\lambda_{max}$ = 495 nm.

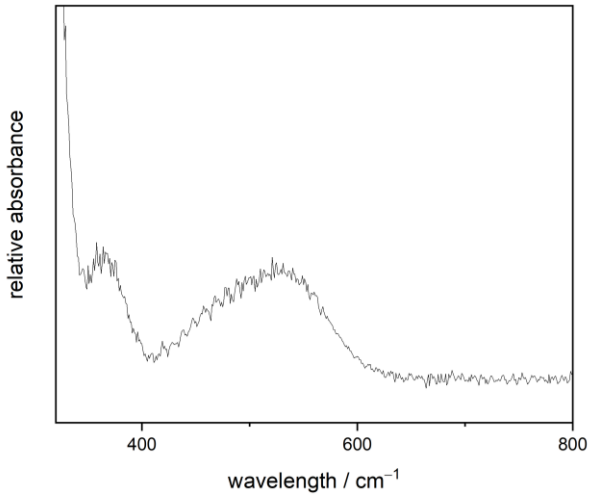


Figure S67. UV/VIS spectrum of [$FeC_{10}DMS_8H_2$] (**4b**) in *n*-pentane. $\lambda_{max}$ = 521 nm.

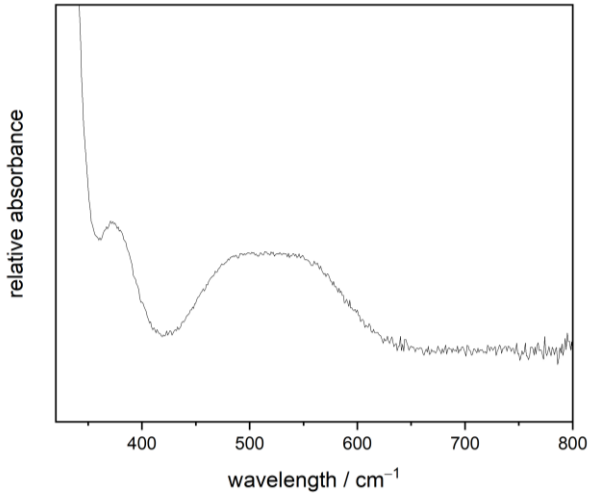


Figure S68. UV/VIS spectrum of [$FeC_{10}DMS_9H$] (**5**) in *n*-pentane. $\lambda_{max}$ = 524 nm.

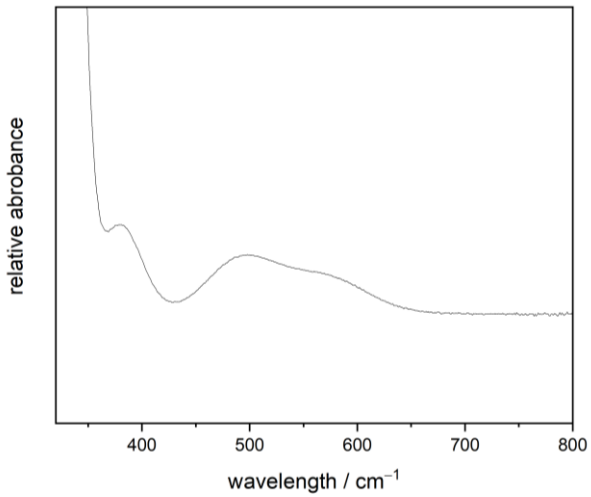


Figure S69. UV/VIS spectrum of [$FeC_{10}DMS_{10}$] (**6**) in *n*-pentane. $\lambda_{max}$ = 500 nm.

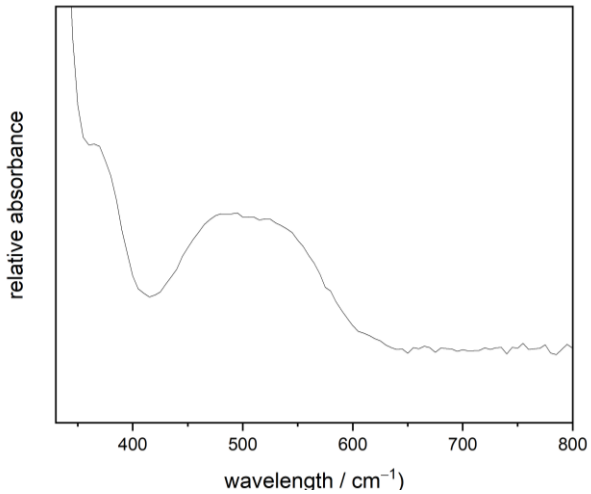


Figure S70. UV/VIS spectrum of [$FeC_{10}DMS_8Me_2$] (**8**) in *n*-pentane. $\lambda_{max}$ = 490 nm.

## 5.5 High Performance Chromatograms

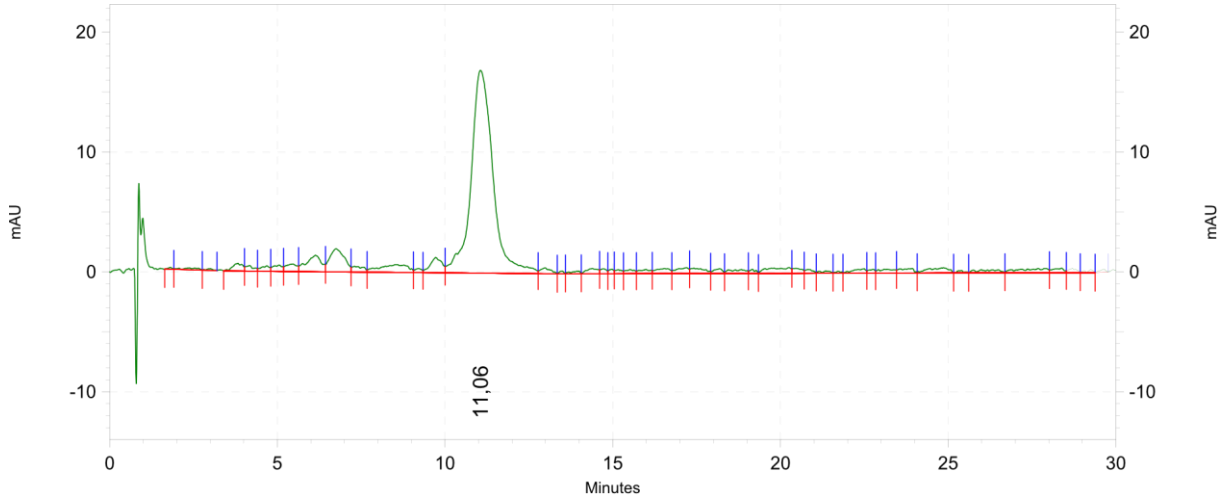


Figure S71. Chromatogram of [$FeC_{10}DMS_9Br$] (**2**). RP-18, MeOH(98%), room temperature.

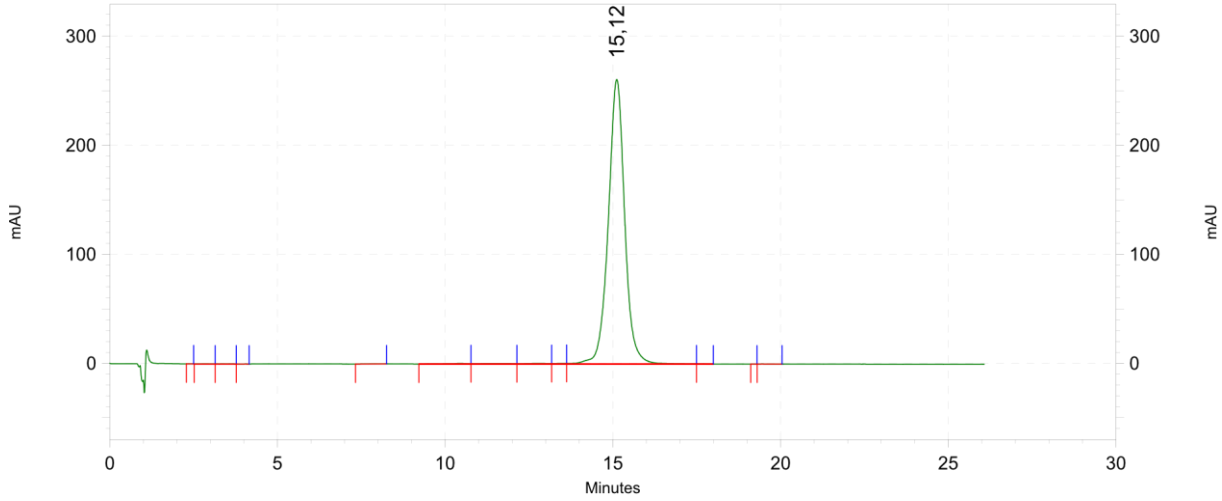


Figure S72. Chromatogram of [$FeC_{10}DMS_8Br_2$] (**1**). RP-18, MeOH(98%), room temperature.

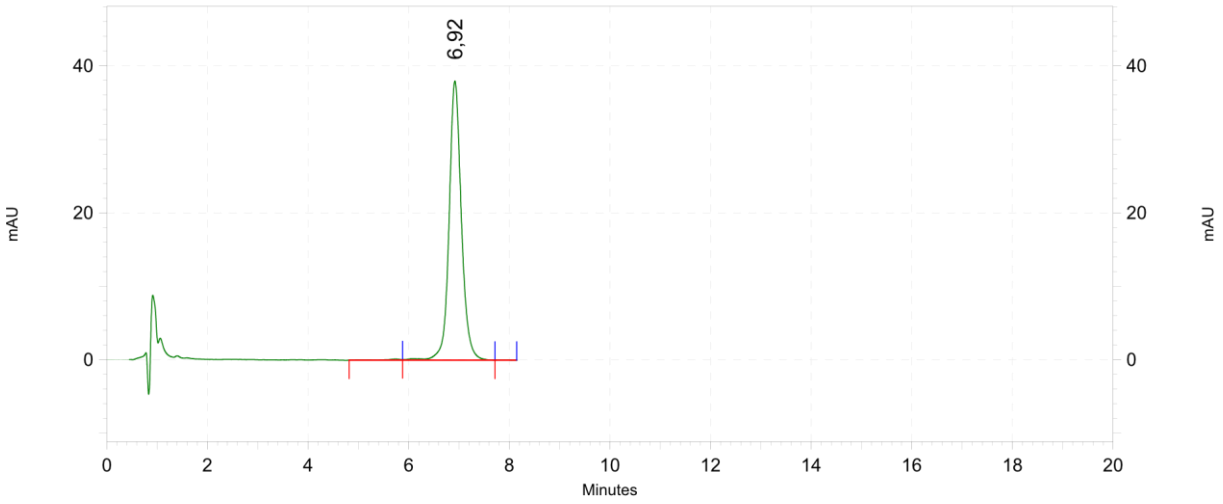


Figure S73. Chromatogram of [$FeC_{10}DMS_7H_3$] (**3a**). RP-18, MeOH(98%), room temperature.

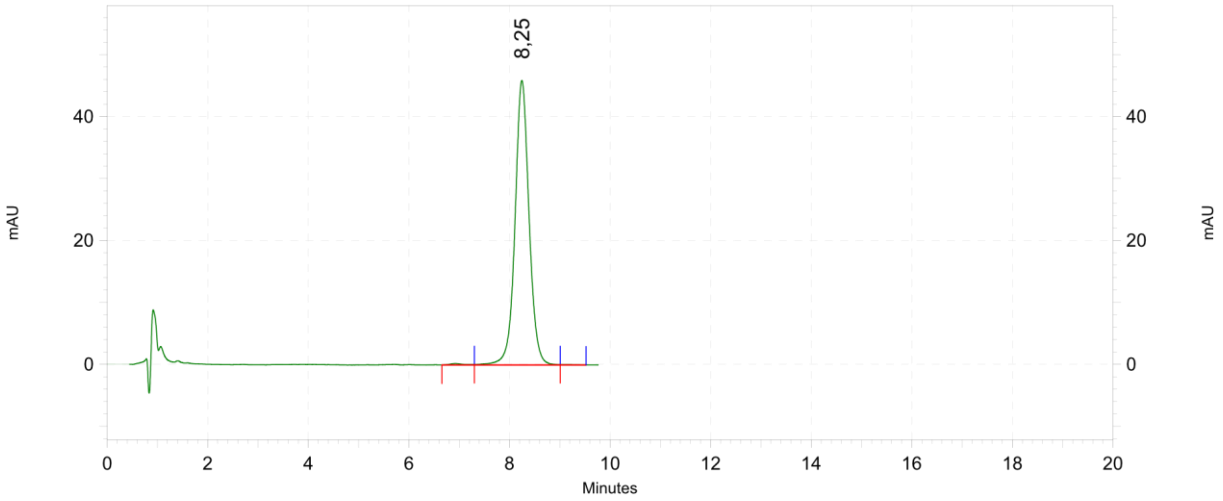


Figure S74. Chromatogram of [$FeC_{10}DMS_7H_3$] (**3b**). RP-18, MeOH(98%), room temperature.

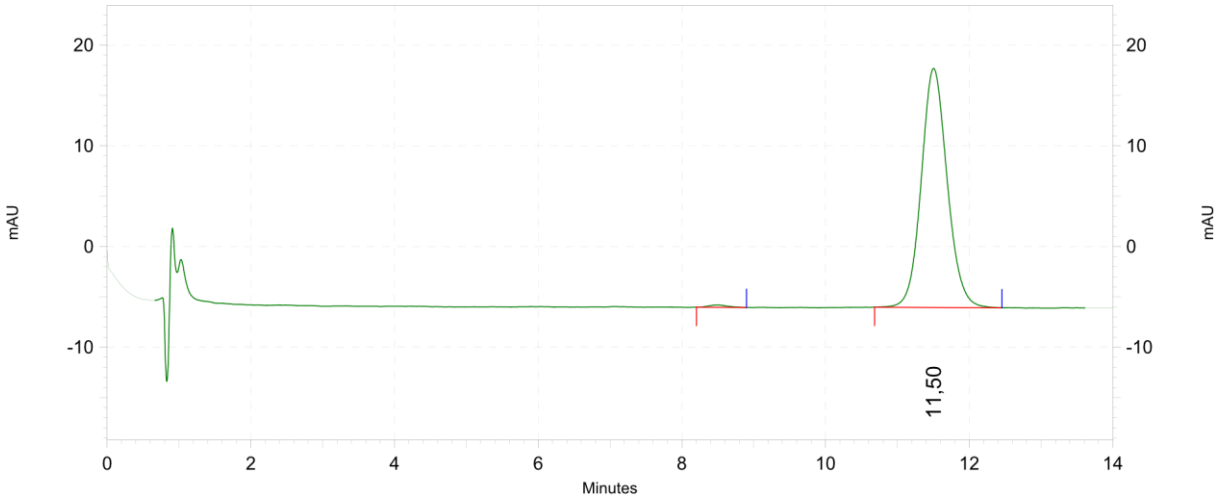


Figure S75. Chromatogram of [$FeC_{10}DMS_8H_2$] (**4a**). RP-18, MeOH(98%), room temperature.

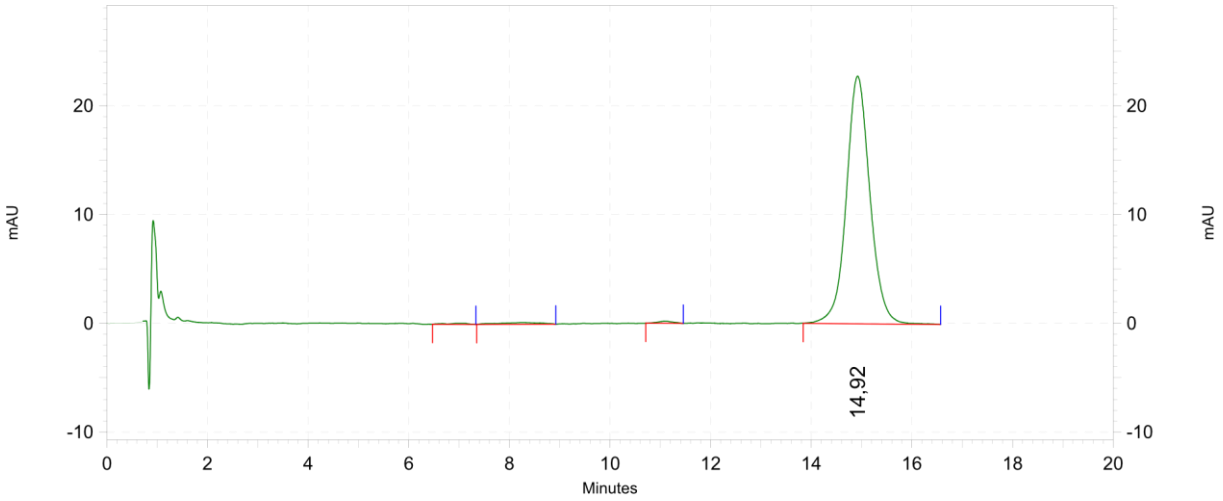


Figure S76. Chromatogram of [$FeC_{10}DMS_8H_2$] (**4b**). RP-18, MeOH(98%), room temperature.

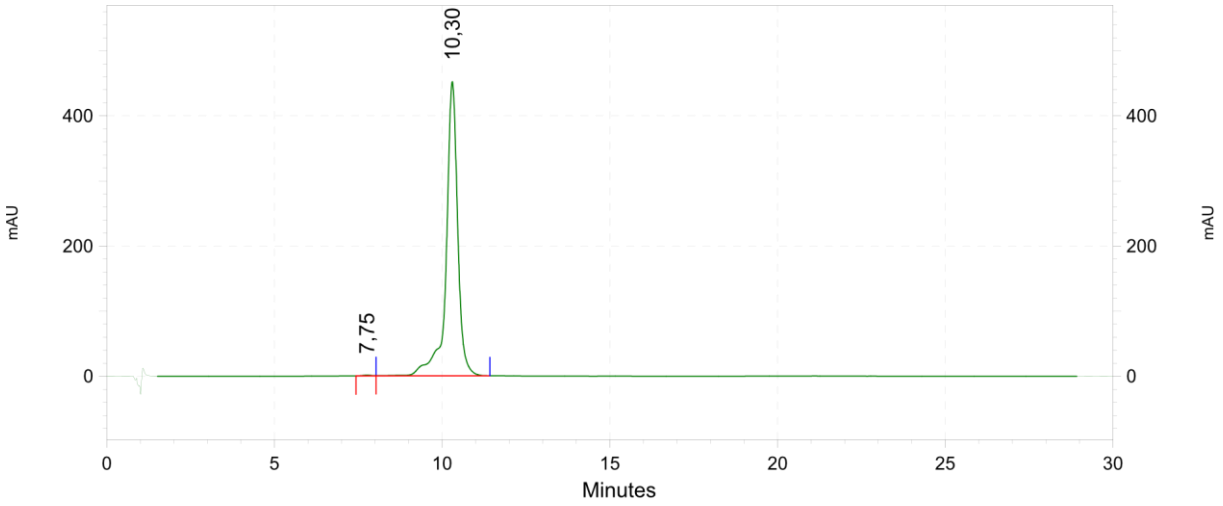


Figure S77. Chromatogram of [$FeC_{10}DMS_9H$] (**5**). RP-18, 9:1 MeOH(98%) and THF, room temperature.

# 5 Computational Details

All calculations were performed using the TURBOMOLE program code, Version 7.6.[14,15] Structures were optimized in the gas phase using the full molecular symmetry and the r$^2$SCAN-3c composite approach with the respective basis sets.[16] All structures were identified as minima of the potential energy surface by numerical frequency calculations.
All UV/vis spectra were calculated with time-dependent density functional theory using the ωB97X-D functional,[17] the def2-TZVPPD basis set[18] and in $C_1$ symmetry. For the species **6**, only a def2-TZVPP basis set was assigned to the DMS groups to improve numerical performance of the excitation energy calculations. For the calculation of UV/vis spectra, solvation effects for *n*-hexane were considered at the COSMO level,[19] using the FINE cavity ($cosmo_isorad),[20] a dielectric constant of 1.92 and a refractive index of 1.3855. The number of excitations was chosen in such a way that the highest excitation in each irreducible representation was above 7.0 eV.

The SCF was converged to energy changes below $10^{-9}$ Hartree and density matrix entry changes below $10^{-7}$. Every calculation used a non-standard grid (gridsize 3, radsize 8). All calculations employed the multipole-accelerated resolution of the identity (MARI-J) approximation[21] in combination with the appropriate auxiliary basis sets.[22] The calculations at the ωB97X-D level also employed semi-numerical exact exchange ($senex)[23] with a gridsize of 1 and de-aliasing. Atomic charges were computed using natural population analysis (NPA).[24]

Table S5. NPA charges and TDDFT results for the positions of the lowest-energy absorption bands (in nm) for [FeCp$_2$], [FeCp$_2$] with the elongated Fe-C distances of **6**, and for persilylated **6.** ωB97X-D/def2-TZVPP(D)/COSMO//r$^2$SCAN-3c data.

| | $q^{NPA}$(Fe) | band 1 | band 2 | band 3 |
|---|---|---|---|---|
| [FeCp$_2$] ($D_{5h}$) | 0.271 | 512 | 461 | 351 |
| [FeCp$_2$] ($D_{5d}$) | 0.276 | 525 | 468 | 355 |
| [FeCp$_2$] ($D_{5h}$) elongated | 0.298 | 654 | 557 | 405 |
| [FeCp$_2$] ($D_{5d}$) elongated | 0.302 | 667 | 563 | 408 |
| [Fe($C_5$DMS$_5$)$_2$] ($D_5$), **6** | 0.301 | 671 | 589 | 423 |
| [Fe($C_5$DMS$_5$)$_2$] ($S_{10}$), **6** | 0.303 | 683 | 595 | 426 |

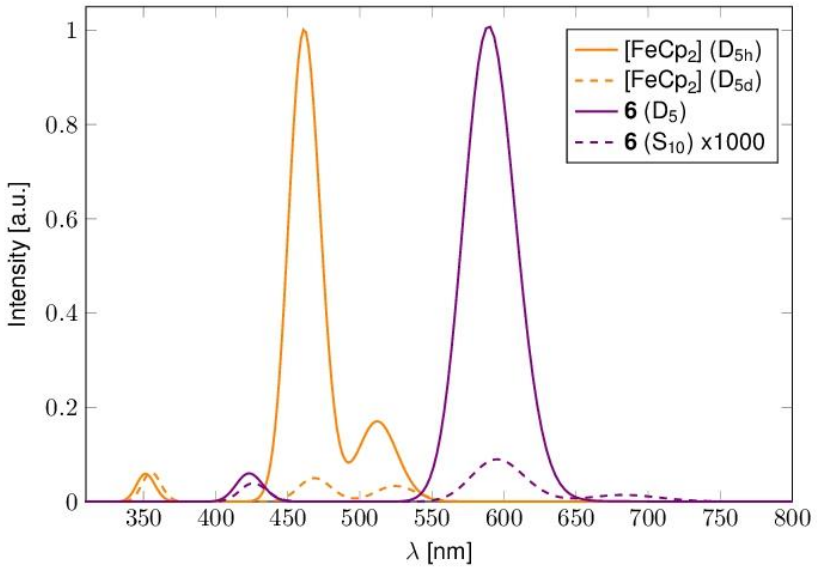


Figure S78. Excitation spectra obtained at TDDFT level (ωB97X-D/def2-TZVPP(D)/COSMO//r2SCAN-3c). Bands were modeled as Gaussians with a width at half maximum of 0.15 eV. The intensities are normalized to 1 for the most intense excitation of each species. The spectrum of the S10 symmetric species of **6** is enhanced by a factor of 1000.

Figure S79. Molecular structure of [$FeC_{10}DMS_{10}$] (**6**) in solid state. Left: asymmetric unit, center: conformer **A** ($D_5$), right: conformer **B** ($S_{10}$). hydrogen atoms are omitted for clarity. Color code: purple – silicon, orange – iron, gray – carbon.

# 6 References


(1) Rupf, S. M.; Dimitrova, I. S.; Schröder, G.; Malischewski, M. Preparation and One-Electron Oxidation of Decabromoferrocene. *Organometallics* **2022**, *41*, 1261–1267.

(2) Rupf, S. M.; Schröder, G.; Sievers, R.; Malischewski, M. Tenfold Metalation of Ferrocene: Synthesis, Structures, and Metallophilic Interactions in $FeC_{10}(HgX)_{10}$. *Chem. Eur. J.* **2021**, *27*, 5125–5129.

(3) Rathman, T. L.; Schwindeman, J. A. Preparation, Properties, and Safe Handling of Commercial Organolithiums: Alkyllithiums, Lithium sec-Organoamides, and Lithium Alkoxides. *Org. Process Res. Dev.* **2014**, *18*, 1192–1210.

(4) Harris, R. K.; Becker, E. D.; Menezes, S. M. C. de; Granger, P.; Hoffmann, R. E.; Zilm, K. W. Further Conventions for NMR Shielding and Chemical Shifts (IUPAC Recommendations 2008). *Pure Appl. Chem.* **2008**, *80*, 59.

(5) Willcott, M. R. MestRe Nova. *J. Am. Chem. Soc.* **2009**, *131*, 13180.

(6) T. H. J., N.; M., S. MMass as a Software Tool for the Annotation of Cyclic Peptide Tandem Mass Spectra. *PLoS One* **2012**, *7*, e44913.

(7) *Origin(Pro), Version 2016*; OriginLab Corporation: Northhampton, Massachusetts, USA, 2016.

(8) Dolomanov, O. V.; Bourhis, L. J.; Gildea, R. J.; Howard, J. A. K.; Puschmann, H. OLEX2: A Complete Structure Solution, Refinement and Analysis Program. *J. Appl. Cryst.* **2009**, *42*, 339–341.

(9) Sheldrick, G. M. Crystal Structure Refinement with SHELXL. *Acta Cryst.* **2015**, *A71*, 3–8.

(10) Sheldrick, G. M. *SHELXL Version 2014/7, Program for Crystal Structure Solution and Refinement*; Göttingen, Germany, 2014.

(11) Sheldrick, G. M. A Short History of SHELX. *Acta Cryst.* **2008**, *A64*, 112–122.

(12) Brandenburg, K. Diamond: Crystal and Molecular Structure Visualization http://www.crystalimpact.com/diamond.

(13) Persistence of Vision Pty. Ltd. Persistence of Vision Raytracer. Ltd., Persistence of Vision Pty. 2004.

(14) *TURBOMOLE Version 7.5 2020*, a Development of University of Karlsruhe and Forschungszentrum Karlsruhe GmbH, 1989-2007, TURBOMOLE GmbH, since 2007; TURBOMOLE GmbH. http://www.turbomole.com (accessed Mar 12, 2023).

(15) Balasubramani, S. G.; Chen, G. P.; Coriani, S.; Diedenhofen, M.; Frank, M. S.; Franzke, Y. J.; Furche, F.; Grotjahn, R.; Harding, M. E.; Hättig, C.; Hellweg, A.; Helmich-Paris, B.; Holzer, C.; Huniar, U.; Kaupp, M.; Khah, A. M.; Khani, S. K.; Müller, T.; Mack, F.; Nguyen, B. D.; Parker, S. M.; Perlt, E.; Rappoport,

D.; Reiter, K.; Roy, S.; Rückert, M.; Schmitz, G.; Sierka, M.; Tapavicza, E.; Tew, D. P.; van Wüllen, C.; Voora, V. K.; Weigend, F.; Wodyński, A.; Yu, J. M. *J. Chem. Phys.* **2020**, *152*, 184107.

(16) Grimme, S.; Hansen, A.; Ehlert, S.; Mewes, J.-M. r$^2$SCAN-3c: A "Swiss army knife" composite electronic-structure method. *J. Chem. Phys.* **2021**, *154*, 064103.

(17) Chai, J.-D.; Head-Gordon, M. Long-range corrected hybrid density functionals with damped atom–atom dispersion corrections. *Phys. Chem. Chem. Phys.* **2008**, *10*, 6615–6620.

(18) Wachters, A. J. H. Gaussian basis set for molecular wavefunctions containing third-row atoms. *J. Chem. Phys.* **1970**, *52*, 1033–1036.

(19) Klamt, A.; Schüürmann, G. COSMO. *J. Chem. Soc., Perkin Trans. 2* **1993**, *2*, 799–805.

(20) Klamt, A.; Diedenhofen, M. A refined cavity construction algorithm for the conductor-like screening model. *J. Comput. Chem.* **2018**, *39*, 1648–1655.

(21) Sierka, M.; Hogekamp, A.; Ahlrichs, R. Fast evaluation of the Coulomb potential for electron densities using multipole accelerated resolution of identity approximation. *J. Chem. Phys.* **2003**, *118*, 9136–9148.

(22) Weigend, F. Accurate Coulomb-fitting basis sets for H to Rn. *Phys. Chem. Chem. Phys.* **2006**, *8*, 1057–1065.

(23) Holzer, C. An improved seminumerical Coulomb and exchange algorithm for properties and excited states in modern density functional theory. *J. Chem. Phys.* **2020**, *153*, 184115.

(24) Reed, A. E.; Weinstock, R. B.; Weinhold, F. Natural population analysis. *J. Chem. Phys.* **1985**, *83*, 735.